IOWA STATE UNIVERSITY
Digital Repository

Graduate Theses and Dissertations

Iowa State University Capstones, Theses and Dissertations

2011

A study of semiconductor photocatalysts for potential environmental remediation processes

Deborah Rose Lipman Chernyshov
Iowa State University

Follow this and additional works at: https://lib.dr.iastate.edu/etd

 Part of the Chemistry Commons

Recommended Citation
Lipman Chernyshov, Deborah Rose, "A study of semiconductor photocatalysts for potential environmental remediation processes" (2011). *Graduate Theses and Dissertations*. 12047.
https://lib.dr.iastate.edu/etd/12047

This Thesis is brought to you for free and open access by the Iowa State University Capstones, Theses and Dissertations at Iowa State University Digital Repository. It has been accepted for inclusion in Graduate Theses and Dissertations by an authorized administrator of Iowa State University Digital Repository. For more information, please contact digirep@iastate.edu.

www.manaraa.com

A study of semiconductor photocatalysts for potential environmental remediation processes

by

Deborah Rose Lipman Chernyshov

A thesis submitted to the graduate faculty

in partial fulfillment of the requirements for the degree of

MASTER OF SCIENCE

Major: Chemistry (Organic Chemistry)

Program of Study Committee:
William S. Jenks, Major Professor
Theresa L. Windus
Nicola Pohl

Iowa State University

Ames, Iowa

2011

www.manaraa.com

Table of Contents

www.manaraa.com

www.manaraa.com

Chapter 1: General Introduction

1.1 THESIS ORGANIZATION

The five chapters of this thesis demonstrate the process by which visible light semiconductor photocatalysts are synthesized and improved upon so that they may be used in environmental remediation. Chapter 1 is a general introduction that reviews semiconductor photocatalysts and how they may be used in environmental remediation.

Chapter 2 is a paper that will be submitted for publication simultaneously with this defense. It examines iodine-modified titanium dioxide's ability to degrade a variety of pollutants under ultraviolet (UV) and visible light irradiation and the pathways used to degrade afore mentioned pollutants. The effects of various annealing temperatures and environments had on the catalyst's characteristics and efficiency are reported.

Chapter 3 is a draft of a paper that will be published shortly. It examines bismuth (III) oxyiodide as a potential visible light photocatalyst. In this paper, the efficiency and robustness of the catalyst is examined and mechanistic pathways are explored in hopes of eliminating discrepancies within the literature and providing realistic expectations of the catalyst in question's abilities.

Chapter 4 is a paper that was published in The Journal of Physical Organic Chemistry in February 2011. It examines a group of potential new probe molecules with similar structures in hopes of determining the regioselectivity of degradative processes and the effect electron density has on this and the method of degradation.

Finally, Chapter 5 draws some general conclusions and examines possibilities for future work in the field of environmental remediation.

1.2 SEMICONDUCTOR PHOTOCATALYSTS

Environmental remediation has become a pressing issue within our society. As our water and air have become more polluted, the need to remove these pollutants has become ever greater.[1] One promising area of study is that of semiconductor photocatalysts. These catalysts

www.manaraa.com

are interesting due to their ability to catalyze reactions that oxidize pollutants when exposed to light in the presence of oxygen. They are also applicable to industry because of their low costs, stability over long periods of use, low toxicity, and ability to be tuned to specific needs and conditions. Though the ideal catalysts is easy to describe: inexpensive to make, stable over long periods of time, and able to degrade a wide variety of pollutants efficiently with little to no energy input from the operator; it has yet to be discovered. [2] It is for this reason that the research presented in this thesis is necessary.

1.3 STRUCTURE AND FUNCTION OF SEMICONDUCTOR PHOTOCATALYSTS

Semiconductors contain a filled lower energy valance band and a higher energy, empty conduction band separated by an energy difference known as a band gap. On absorption of a photon of sufficient energy (greater than or equal to that of the band gap) an electron is promoted to the conduction band, leaving behind a positive hole in the valance band.[3] As shorter wavelengths of light have more energy, ultraviolet light is required to excite electrons in catalysts with large band gaps while catalysts with smaller band gaps may become activated by visible light irradiation.

Altering the size of the band gap can occur through doping, the purposeful introduction of impurities into the crystal lattice. Once introduced, these impurities can introduce mid-gap states, or energy levels that exist within the semiconductors band gap, where no states normally exist. The introduced states can be either filled or empty and can lie just below the conduction band or slightly above the valance band depending on the type of dopant used, but they all decrease the amount of energy required to create electron-hole pairs by decreasing the amount of energy required to excite the electrons as depicted in Figure 1.1.[3]

www.manaraa.com

Figure 1. Schematic drawing of a semiconductor containing mid-gap states introduced by a dopant. Note: unless doubly doped, only one introduced state is likely to exist, not both.

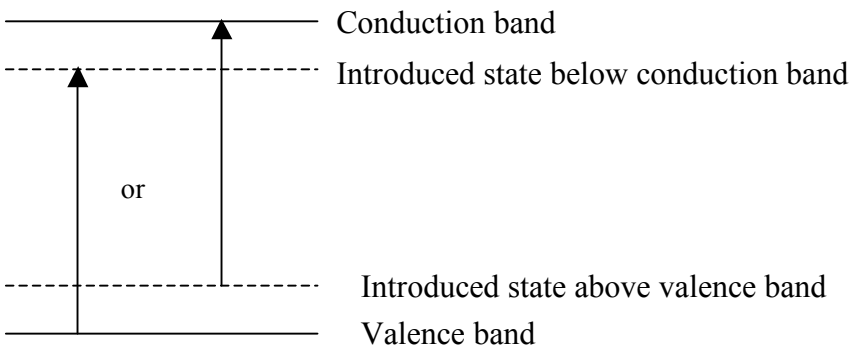

In addition to the mid-gap states introduced by the dopants, crystal defects can be formed, often in the form of oxygen vacancies. These defects may also be responsible for the increased visible light absorption of doped catalysts,[4] and are important, especially for titanium dioxide, because they not only increase visible light absorption, but also govern oxygen adsorption, which is critical to the photocatalytic ability of the catalysts because of oxygen's role as an electron scavenger and oxidizer of organic molecules on the surface of the catalyst.[5]

Regardless of what causes visible light absorption or which wavelengths are absorbed, once excitation occurs (Equation 1.1), the same series of reaction pathways- it is presumed- may occur. The least desired reaction is recombination of the electron and hole, in which no chemical reaction occurs because a hole and an electron react to give off heat and/or light. (Equation 1.2) Another potential reaction is that of an electron reacting with molecular oxygen to form superoxide, and eventually hydroxyl radicals, which can potentially degrade pollutants or cause other chemical reactions to occur. (Equation 1.3 - 1.8) Finally, the hole left in the valance band can react with either water or hydroxide anions to produce adsorbed hydroxyl radicals or with an organic substrate (S) in what is know as a single electron

www.manaraa.com

transfer (SET) reaction, which also lead to degradation of the pollutants. (Equations 1.9 – 1.11)[6-9]

$$TiO_2 + h\nu \rightarrow e^-_{cb} + h^+_{vb} \quad (1.1)$$

$$e^-_{cb} + h^+_{vb} \rightarrow \text{heat and/or light} \quad (1.2)$$

$$e^-_{cb} + O_2 \rightarrow O_2^{\bullet -} \quad (1.3)$$

$$O_2^{\bullet -} + H^+ \rightarrow HOO^{\bullet} \quad (1.4)$$

$$HOO^{\bullet} + e^- \rightarrow HOO^- \quad (1.5)$$

$$HOO^- + H^+ \rightarrow H_2O_2 \quad (1.6)$$

$$H_2O_2 + h\nu \rightarrow 2\ {}^{\bullet}OH \quad (1.7)$$

$$H_2O_2 + e^- \rightarrow {}^-OH + {}^{\bullet}OH \quad (1.8)$$

$$H_2O + h^+_{vb} \rightarrow {}^{\bullet}OH_{ads} + H^+ \quad (1.9)$$

$${}^-OH + h^+_{vb} \rightarrow {}^{\bullet}OH_{ads} \quad (1.10)$$

$$S + h^+_{vb} \rightarrow S^{\bullet +} \quad (1.11)$$

Which reaction(s) occur is based on three main factors. First, the energy required for the reaction must be less than that of the band gap, and secondly, the redox potentials of the electrons and holes must be negative and positive enough respectively to promote redox reactions within the substrates, oxygen, water, or hydroxide ions. This makes it inherently difficult to create a catalyst that requires small amounts of excitation energy, such as that provided by sunlight, to be a robust. Finally, the rate of the external reactions must be able to compete with the rate of internal recombination,[2] which is an obvious problem and leads to even the best photocatalysts having a relatively low quantum yield, the ratio of product produced to the number of photons absorbed.[7,10]

www.manaraa.com

It is necessary to determine which degradation pathway is used by the photocatalysts so that predictions can be made as to which substrates will be degraded by the catalysts and how efficiently; it is also useful in predicting reaction intermediates that may be more toxic than the starting substance.[11,12] To determine which of the two main species responsible for substrate degradation, hydroxyl radicals and/or holes (SET chemistry) or to a lesser extent, superoxide, is used by each catalyst, several experimental methods have been developed.

One popular method is to use scavengers, molecules that react with a certain species, hole, hydroxyl radical, etc, to form a stable product that can be identified and quantified.[7] By comparing the rate of degradation of a probe molecule when the scavenger is present and comparing it to the rate of degradation when the scavenger is not present, inferences into what role that species plays in the degradation of the probe can be made. For example, a hydroxyl radical scavenger, such as *tert*-butanol should greatly decrease the rate of degradation for a probe molecule if the probe is degraded by hydroxyl radicals, but will not alter its rate if the probe is degraded through SET chemistry. [13] This however is not always definitive as a hole scavenger could reduce the rate of degradation not only because it is blocking SET chemistry from occurring, but it is also preventing the oxidation of water to hydroxyl radicals. For this reason, when determining degradation pathways through the use of scavengers, it is imperative that the proper controls, and ideally, a variety of scavengers be used.

Another experimental procedure for determining degradation pathways that is similar to the use of scavengers uses a scavenger that luminesces upon reaction with a hydroxyl radical.[7] In this method, a substance, often terphthalic acid, is added to the reaction mixture so that it may react with hydroxyl radicals to form a luminesent product, whose concentration can then be tracked. This shows definitively whether or not hydroxyl radicals are formed. [13] Unfortunately, knowing that hydroxyl radicals are formed does not necessarily indicate that hydroxyl chemistry is the main pathway by which the probe is degraded.

For a more definitive answer on the question of mechanisms, the use of probe molecules that produce specific products based on their mode of degradation are required. Several such probes exist, such as quinoline[11,14] and *p*-aniylneopentanol.[15,16] Though these probes

www.manaraa.com

demonstrate which pathway they underwent while degrading, sometimes they form in very low concentrations and degrade quickly making their identification and quantification difficult. To manage this problem, the probe's concentration is often elevated so that the small amount of intermediate formed will be detectable, but this in its self could alter the reaction mechanism.[12] Though no one experimental procedure is fail-proof, using them in conjunction with each other can lead to a thorough understanding of the catalyst's chemical workings.

Finally, approximate values for the redox potentials of the holes/electrons may be calculated and compared to the potentials of water, hydroxide anions, and oxygen to determine if hydroxyl radicals can be formed through the oxidation of water or hydroxide anions or through the reduction of oxygen to produce superoxide.[17] However, when considering the possibility of reducing oxygen, it must be remembered that the calculated reduction potential is calculated for the lowest energy conduction band state and can therefore erroneously be used to disregard the possibility of superoxide formation prematurely as it may appear that the reduction of oxygen is impossible when in fact higher energy states that can reduce oxygen may exist.[18] For this reason, these calculations must be used with caution and should be done in conjunction with experimental analysis.

1.4 TITANIUM DIOXIDE AS A SEMICONDUCTOR PHOTOCATALYST

Titanium dioxide is one of the most studied semiconductor photocatalysts, and its ability to degrade a variety of pollutants efficiently is well documented.[2,19,20] However, due to its band gap of 3.2 eV, it can only absorb wavelengths below about 387 nm, UV light, which accounts for only about 5% of the solar spectrum.[21] This means that UV lights must be installed and used to activate TiO_2, rather than making use of free ambient light. For this reason, scientists hope to synthesize a TiO_2 species that will be active under solar light irradiation.

In attempts to create a solar light active TiO_2 species, many efforts have been made to move its absorption edge into the visible region,[21] which accounts for approximately half of the solar spectrum.[22] Some of the earlier efforts involved doping TiO_2 with metals and eventually transition metals.[2,21,23-25] Though these doped species originally showed great

www.manaraa.com

promise as they absorbed into the visible region, further study showed that they had two major flaws: decreased thermal and chemical stability and increased e^-/h^+ recombination rates. The dopants themselves acted as recombination centers.[4,7,21,26] Thus, the doped catalysts were often less efficient even though they absorb visible light, and due to the lower energy states they contained, they often had less oxidative ability than unmodified catalysts making them less robust.[26]

Because metal doped TiO_2's problems have been difficult to overcome, nonmetal dopants[2,16,19,27] have begun being used to enhance visible light activity. Though these dopants suffer less from the problems that have plague the metal doped catalysts, they are not perfect. It is known that as the band gap is decreased, the oxidative ability of the catalysts also decreases,[28] meaning that the doped TiO_2 catalysts that absorbs visible light are inherently less robust than TiO_2 itself.

The fact that visible light absorption is not indicative of visible light activity necessitates that new catalysts are studied in detail to determine how efficient and robust they are. To date, many studies of iodine dope titanium dioxide's efficiency have been published, but few detailed studies of mechanistic behavior have been made, and even fewer probe molecules have been tested.[21,27,29] For this reason, the author of this thesis has used probe molecules to study the degradation pathways of iodine modified TiO_2. In an attempt to elucidate the degradation pathways used by the catalysts and the variety of pollutants it may be capable of degrading.

1.5 BISMUTH OXYIODIDES AS SEMICONDUCTOR PHOTOCATALYSTS

Due to the problems encountered in improving titanium dioxide catalysts, several researchers have begun to study bismuth oxyhalides, and in particular bismuth oxyiodide, as potential visible light photocatalysts. Primary studies of bismuth oxychloride and oxybromide have suggested that they are highly efficient photocatalysts, capable of degrading certain probe molecules more rapidly than P25, the standard titanium dioxide species that is used as a benchmark for other photocatalysts, under the same conditions. Though bismuth oxychloride cannot absorb visible light, both bismuth oxybromide and

www.manaraa.com

oxyiodide are known to be visible light active without further modifications and treatments, with bismuth oxyiodide being highly efficient under visible light and artificial solar light irradiation. [21,30,31] For this reason, the author of this thesis has focused their research on bismuth oxyiodide.

Though bismuth oxyiodide shows promise as an emerging photocatalyst and has been shown to be highly effective in degrading both selected aqueous[1,13,32] and gaseous[33] model pollutants, most of these studies have used the same or very similar probe molecules so the diversity of pollutants that can be degraded by bismuth oxyiodide is unknown. Also, and possibly more importantly, little is known about the catalyst mechanistically. There are a few studies in the literature that have tried to elucidate the degradation pathways used by catalyst. Most claim that hydroxyl radicals are not formed, and that therefore SET chemistry must be responsible for the degradation of pollutants, but they are inconsistent when it comes to the role superoxide plays.[13,17,31] Therefore, further studies into the mechanistic pathways used by these catalysts and their robustness are necessary.

1.6 REFERENCES

(1) Yu, C.; Fan, C.; Yu, J. C.; Zhou, W.; Yang, K. *Mater. Res. Bull.* **2011**, *46*, 140.

(2) Chatterjee, D.; Dasgupta, S. *Journal of Photochemistry and Photobiology C: Photochemistry Reviews* **2005**, *6*, 186.

(3) Close, K. J.; Yarwood, J. *An Introduction to Semiconductro Electronics*; 2nd ed.; Heinemann Educational Books Ltd: London, 1982.

(4) Emeline, A. V.; Sheremetyeva, N. V.; Khomchenko, N. V.; Ryabchuk, V. K.; Serpone, N. *The Journal of Physical Chemistry C* **2007**, *111*, 11456.

(5) Thompson, T.; Yates, J. *Topics in Catalysis* **2005**, *35*, 197.

(6) Dodd, N. J. F.; Jha, A. N.

(7) Pichat, P. *Water Science & Technology* **2007**, *55*, 167.

(8) Oh, Y.-C.; Li, X.; Cubbage, J. W.; Jenks, W. S. *Applied Catalysis B: Environmental* **2004**, *54*, 105.

www.manaraa.com

(9) Emeline, A. V.; Ryabchuk, V. K.; Serpone, N. *The Journal of Physical Chemistry B* **2005**, *109*, 18515.

(10) Suppan, P. *Principles of photochemistry*; Chemical Society: London, 1973; Vol. 22.

(11) Li, X.; Cubbage, J. W.; Jenks, W. S. *Journal of Photochemistry and Photobiology A: Chemistry* **2001**, *143*, 69.

(12) Pichat, P. *Water Sci. Technol.* **1997**, *35*, 73.

(13) Li, Y.; Wang, J.; Yao, H.; Dang, L.; Li, Z. *Journal of Molecular Catalysis A: Chemical* **2011**, *334*, 116.

(14) Cermenati, L.; Albini, A.; Pichat, P.; Guillard, C. *Research on Chemical Intermediates* **2000**, *26*, 221.

(15) Hathway, T.; Jenks, W. S. *Journal of Photochemistry and Photobiology A: Chemistry* **2008**, *200*, 216.

(16) Rockafellow, E. M.; Stewart, L. K.; Jenks, W. S. *Applied Catalysis B: Environmental* **2009**, *91*, 554.

(17) Chang, X.; Huang, J.; Tan, Q.; Wang, M.; Ji, G.; Deng, S.; Yu, G. *Catalysis Communications* **2009**, *10*, 1957.

(18) Jiang, Z.; Yang, F.; Yang, G.; Kong, L.; Jones, M. O.; Xiao, T.; Edwards, P. P. *Journal of Photochemistry and Photobiology A: Chemistry* **2010**, *212*, 8.

(19) Fujishima, A.; Zhang, X.; Tryk, D. A. *Surface Science Reports* **2008**, *63*, 515.

(20) Gaya, U. I.; Abdullah, A. H. *Journal of Photochemistry and Photobiology C: Photochemistry Reviews* **2008**, *9*, 1.

(21) Hong, X.; Wang, Z.; Cai, W.; Lu, F.; Zhang, J.; Yang, Y.; Ma, N.; Liu, Y. *Chem. Mater.* **2005**, *17*, 1548.

(22) Przyborski, P.; Remer, L.; Vol. 2011.

(23) Matsumoto, Y.; Katayama, M.; Abe, T.; Ohsawa, T.; Ohkubo, I.; Kumigashira, H.; Oshima, M.; Koinuma, H. *Journal of the Ceramic Society of Japan* **2010**, *118*, 993.

(24) Eslava, S.; McPartlin, M.; Thomson, R. I.; Rawson, J. M.; Wright, D. S. *Inorganic Chemistry* **2010**, *49*, 11532.

www.manaraa.com

(25) Vu, A. T.; Nguyen, Q. T.; Bui, T. H. L.; Tran, M. C.; Dang, T. P.; Tran, T. K. H. *Advances in Natural Sciences: Nanoscience and Nanotechnology* **2010**, *1*, 015009/1.

(26) Serpone, N.; Lawless, D.; Disdier, J.; Herrmann, J.-M. *Langmuir* **1994**, *10*, 643.

(27) Su, W.; Zhang, Y.; Li, Z.; Wu, L.; Wang, X.; Li, J.; Fu, X. *Langmuir* **2008**, *24*, 3422.

(28) Grassian, V. H. *Environmental catalysis*; Taylor & Francis/CRC Press: Boca Raton, FL, 2005.

(29) Tojo, S. T., T.; Fujitsuka, M.; Majima, T. *J. Phys. Chem. C* **2008**, *112*, 14948.

(30) Zhang, X.; Ai, Z.; Jia, F.; Zhang, L. *The Journal of Physical Chemistry C* **2008**, *112*, 747.

(31) Chang, X.; Huang, J.; Cheng, C.; Sui, Q.; Sha, W.; Ji, G.; Deng, S.; Yu, G. *Catalysis Communications* **2010**, *11*, 460.

(32) Zhang, X.; Zhang, L.; Xie, T.; Wang, D. *J. Phys. Chem. C* **2009**, *113*, 7371.

(33) Ai, Z.; Ho, W.; Lee, S.; Zhang, L. *Environmental Science & Technology* **2009**, *43*, 4143.

www.manaraa.com

Chapter 2: Iodine doped titanium dioxide: A case study of catalytic activity based on annealing conditions

*Deborah R. Lipman Chernyshov, Jessica Haywood, Erin M. Rockafellow, William S. Jenks**

Department of Chemistry, Iowa State University, Ames, IA 50011-3111, United States

This is a preliminary version of the paper that will be submitted for publication in ACS *Catalysis*. The author of this thesis is responsible the experimental results found within the paper with the following exceptions. Jessica Haywood synthesized the amorphous TiO_2 and annealed several samples in addition to performing the point of zero charge experiments. Jessica Haywood and Erin A. Rockafellow obtained some of the XPS and UV/Vis spectra contained within the paper, and the author of this thesis would also like to thank Erin A. Rockafellow for her experimental and conceptual assistance throughout the creation of this paper.

2.1 ABSTRACT

Iodine modified TiO_2 catalysts were synthesized using the method first described by Hong, *et al.*[1] The amorphous material was annealed at various temperatures and under oxidizing and non-oxidizing atmospheres. Though varying the annealing temperatures altered the oxidation state of iodine present in the catalyst, with low temperatures giving I^{7+}/I^{5+} and high temperatures giving I^-, the annealing environment had no effect. The chemistry of the resulting catalysts was evaluated using various probe molecules (quinoline, *p*-anisylneopentanol, formic acid, and phenylacetic acid) chosen because they reveal mechanistic information on the oxidations. Though the catalysts' UV efficiency was decreased, several showed modest visible light activity when degrading quinoline. While most exhibited single electron transfer (SET) chemistry under visible light irradiation, a few reacted via hydroxyl chemistry, possibly making them better suited to degrade pollutants which are not inclined to SET chemistry. The catalyst that had been annealed at 600 ˚C under nitrogen (ITi 600 N) contained no iodine after annealing but looked the same as its iodine containing counterpart, which was annealed at 600 ˚C in air (ITi 600). ITi 600 N also

www.manaraa.com

degraded pollutants at rates similar to its doped counterpart, not TiO_2. This supports claims that oxygen vacancies and crystal defects are responsible for visible light absorption and catalytic activity, not dopants.

2.2 INTRODUCTION

As people have become more aware of organic pollutants' impact on the environment, legislation and public outcry have made it necessary to find efficient, eco-friendly, and cost effective methods for pollutant remediation. Ideally, degradation catalysts would be non-toxic, inexpensive, and efficient. One of the most promising and exhaustively studied areas is that of heterogeneous photocatalysis.[2] A solid photocatalyst could be secured to a support, placed in contaminated waste water or air flow and through solar irradiation catalyze reactions with organic pollutants until they are mineralized, after which the support and the attached catalyst could be removed.[3,4]

One of the most promising photocatalysts is titanium dioxide (TiO_2) because it inexpensive, robust, non-toxic, and efficient under ultraviolet (UV) irradiation.[2] Unfortunately, UV radiation accounts for only some 5% of the solar spectrum rendering normal TiO_2 catalysts inefficient.[5] To solve this problem, doping of the TiO_2 catalyst, that is the addition of other ions, metals, and nonmetals, has been performed. Doping the TiO_2 with other elements increases the adsorption of visible light, permitting the catalyst to be photoactive under solar light irradiation.[3,6] However, catalysts that absorb visible light are not necessarily superior to their unmodified counterparts. Dopants can often increase recombination, which reduces efficiency, and decreasing the band gap, which permits adsorption of visible light, also lessens the oxidative power of the catalyst, potentially making it less able to degrade a wide variety of pollutants.[7-9]

We have synthesized iodine doped TiO_2 (I-TiO_2) using a modified version of the method described by Xiaoting Hong *et al*. I-TiO_2 appears to be a highly efficient photocatalyst because of its ability to degrade phenol under visible light irradiation ($\lambda > 400$ nm) when annealed at 400 ˚C. Additionally, it has been shown to degrade phenol under UV irradiation with the same efficiency as P-25.[5]

www.manaraa.com

It is important to understand how synthesized photocatalysts degrade pollutants and what properties effect their efficiency so that we may learn how to improve them and be able to make educated predictions as to which other molecules they will be able to degrade and how. For this reason, we have attempted to enhance our understanding of I-TiO_2's degradation mechanisms by using additional probes such as quinoline (Q)[10,11] and *p*-anisylneopentanol (AN)[10,12] that have been shown to produce certain early degradation products that are diagnostic of the degradation mechanism and probes such as formic acid and phenylacetic acid (PAA) which have been shown or are expected to prefer single electron transfer chemistry as shown in Chart 1.[13,14]

Chart 1. Early photocatalytic degradation products for Q, AN, and PAA.

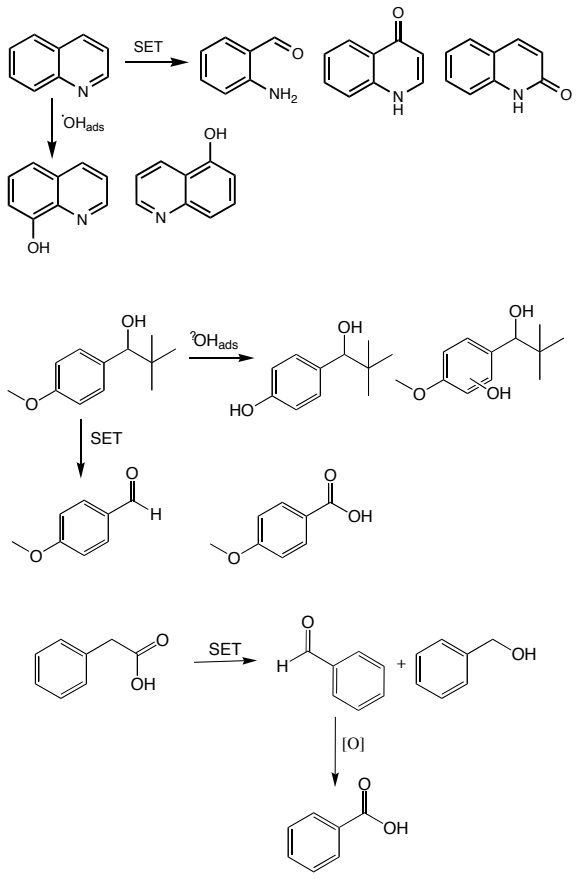

In addition to the three annealing temperatures first explored by Hong[5], 400 °C, 500 °C, and 600 °C, we have also examined the effects of the atmosphere under which annealing occurred. We have annealed the catalysts under both oxidizing and non-oxidizing

www.manaraa.com

atmospheres using air and nitrogen respectively. We hoped to shed light on the reaction mechanisms that take place on or near the surface of I-TiO_2 and to see if these mechanisms varied based on annealing environment and temperature so that we can have a better understanding of how this visible light active catalyst works and in what ways we may be able to improve upon it.

2.3 EXPERIMENTAL

Materials

All chemicals were purchased at reagent grade or higher and used without further modifications unless otherwise noted. AN was prepared using literature methods.[12,15] The water used in all experiments and to make standards for the TOC 5000-Analyzer was purified using a Milli-Q UV plus system and was found to have a resistance of 14.5 MΩ/cm or higher.

Preparation of the photocatalysts

I-TiO_2 was produced using a modified version of the sol-gel method first described by Hong, *et al.*[5] A 4:1 molar ratio of titanium (IV) isopropoxide to iodic acid was used. The necessary amount of iodic acid was dissolved in water to give a 0.15 M solution. To this solution, the correct amount of titanium (IV) isopropoxide was added via a dropping funnel at a rate of ~1.5 mL min^{-1}. As the mixture stirred a white precipitate was formed. Once addition was complete, the white solid was transferred to a beaker and dried at 70 ˚C for 48 hours prior to annealing. After drying, the pre-annealed material was found to have a pale yellow color. As a comparison, undoped material (TiO_2) was also prepared using the same method, less the iodic acid. Sulfur doped titanium dioxide (S-TiO_2) was also used as a comparison catalysts. It was synthesized using a modified version of the procedure described by Ohno. [16-18]

Once dried, the obtained powders were annealed. Three main annealing temperatures, 400 ˚C, 500 ˚C, or 600 ˚C, and two annealing atmospheres, air and nitrogen, were used to create unique catalysts for study. To anneal in air, 1 - 1.5 grams of the dried material was placed in

www.manaraa.com

each sample well of the tube furnace. The samples were then annealed for two hours at the desired temperature with heating and cooling performed as quickly as possible (rate of 99.99 $^{\circ}C\ min^{-1}$). Samples annealed for a longer period of four hours were also examined, but they did not appear to exhibit any unique properties and were discontinued.

To examine the effect of annealing in a non-oxidizing atmosphere, 1 - 1.5 g samples were placed in sample wells and loaded into a quartz tube situated in the tube furnace. The tube that contained the samples was then closed leaving only a small opening for venting and purged for approximately 30 min with nitrogen prior to the start of annealing and throughout the annealing process till the furnace had cooled to below 300 ˚C.

After annealing, the samples were washed by placing them in vials filled with water and permitting them to stir overnight or longer. They were then filtered and allowed to dry overnight in an oven at 70 ˚C prior to use in photocatalytic experiments. Unmodified TiO_2 was annealed at all three temperatures in air for comparison.

The UV/Vis spectra of the catalysts were obtained on an UV/Vis spectrometer that was equipped with a diffuse reflectance accessory using magnesium oxide as a background. XPS data for the catalysts were obtained using a PHI model 5500 multitechnique spectrometer, which used nononochromatized Al-K radiation. The sampling area was 1 mm^2 with a fixed take off angle of 45˚. The peaks were calibrated to the $Ti_{2p3/2}$ peak at 458.8 eV.

To determine the point of zero charge for each catalyst, the potentiometric mass titration technique described by Vakros *et al*. was used.[19] A pH 10-12 solution was made by adding 200 μL of 1 M NaOH to 500 mL of 0.03 M KNO_3.100 mL of this solution was then added to three flasks containing 0.15 g, 0.25 g, and 0.50 g of catalyst respectively. The flasks were then stirred and purged with argon for 1 hr prior to titrating with 100 μL aliquots of HNO_3. Graphing the pH against the volume of acid added and determining where the three lines intersect determined the point of zero charge.

www.manaraa.com

Photocatalytic degradations

All degradations that were performed under UV irradiation were done using a Rayonet minireactor equipped with 8 x 350 nm broad range 4W bulbs unless stated otherwise. Visible light reactions were performed using a Hanovia lamp light source equipped with a 0.5% $K_2Cr_2O_7$ filter, which was tested several times and found to cut off $\lambda < 480$ nm. Two HPLCs were used for data collection, a Varian prostar equipped with a C18 column and photodiode array detector and an HP 1050 equipped with a C18 column and photodiode array detector. The water used in all procedures was distilled deionized water purified with a Millipore Milli-Q system and was found to have a resistance of 14.5 MΩ or more.

Photocatalytic degradation of quinoline was performed using a modified method first developed by Pichat et al. and later used by our group.[20,21] A final catalyst concentration of 1.1 mg L^{-1} was used for all photolyses. The reaction mixtures were prepared by adding 75 mg of catalyst to 35 mL DW. The slurry was then sonicated for 10 minutes to disperse large aggregates before the reaction vessel was wrapped in aluminum foil and 35 mL of 0.3 mM quinoline stock solution was added. The pH was then adjusted to either pH 3 ± 0.5 or pH 6 ± 0.5 using 0.1 M NaOH, 0.1 M HCl, or 0.1 M HNO_3 and the solution was allowed to equilibrate for 30 minutes. Oxygen purging was then begun 15 minutes prior to photolysis and allowed to continue throughout the photolysis. It has been suggested that the Cl^- ion may alter the efficiency of the photocatalyst so HNO_3 was used in a majority of the photolyse; however no significant difference was seen in trials that used HCl.[22,4]

At designated time points, 1.5 mL was removed through a needle. Of that, 1.00 mL was isolated and acidified with 10.0 μL of 1 N H_2SO_4. The sample was then centrifuged, passed through a 0.2 μm filter, and stored at room temperature in the dark till analysis was performed. Kinetic samples were analyzed on the HP 1050 HPLC with an eluent of 25:75 methanol : water mixture and flow rate of 0.9 mL min^{-1}. Products were identified on the Varian Prostar HPLC. 2-aminobenzaldehye, 2-quinolinone, and 4-quinolinone were identified using a 25:75 methanol : water eluent with a flow rate of 1.1 mL min^{-1}. 5-hydroxyquinoline and 8-hydroxyquinoline were identified using a 10:90 methanol : water

www.manaraa.com

eluent, flow rate of 0.75 mL min^{-1}. Products were identified by comparison to authentic samples and were quantified by using the response they evoked from the HPLC detector.

For degradations that were run under argon, the same procedure of sonication and equilibration was used. Instead of purging with oxygen, ~8 mL samples were placed in sealed test tubes and purged with argon for 15-30 min prior to being photolyzed using a the previously described Rayonet minirayonet equipped with a merry-go-round. When a time point was needed, the test tube was removed and a 1.00 mL sample was taken, acidified, centrifuged, and filtered as previously described. The remaining solution was then discarded as air had contaminated the test tube.

Quinoline's primary degradation products were degraded and identified using the same method employed to degrade quinoline. The only difference was that the each product was present in the stock solution in a concentration of 1 mM. 6 mL of stock solution was added to 64 mL deionized water to give a each probe a starting concentration of ~ 0.009 mM.

As a control, co-degradations of phenol and quinoline were run. These degradations used a catalyst concentration of 1 mg mL^{-1}, 0.11 mM phenol, and 0.12 mM quinoline with a total volume of 100 mL. The pH was adjusted with NaOH or HNO_3 as needed to maintain pH 6 +/- 0.5. Samples were taken and treated using the same method as quinoline samples. The kinetics of quinoline were determined using the previously discussed HPLC technique. To monitor the loss of phenol, the samples were analyzed using the HP 1050 HPLC with an eluent of 1:1 water (0.5% acetic acid) and methanol and a flow rate of 0.6 mL min^{-1}. The light source used in these photolyses was a Xenon arc lamp equipped with a 435 nm long pass filter. To maintain ambient temperature, a water IR filter and 2 electric fans were employed.

UV degradations of formic acid[13] were performed with a final catalyst concentration of 0.2 g L^{-1} and reaction volume of 100 mL. Reaction mixtures were prepared by placing 20 mg of catalyst in 10 mL deionized water and sonicating the slurry for 10 minutes to disperse aggregates. After sonication, the reaction vessel was covered with aluminum foil and 90 mL of 20 mM formic acid stock solution was added. Oxygen was purged through the reaction

www.manaraa.com

mixture while it was allowed to equilibrate for 30 min and throughout the photolysis. All degradations were done at natural pH, meaning that no adjustment was performed throughout the photolysis.

Visible light photolyses were performed following the same procedure as the UV photolyses except that the initial concentration of formic acid was ~0.016 mM. This concentration was achieved by dispersing the catalyst in 48 mL DI and adding 2 mL of 0.53 mM probe.

To determine the kinetics of the reaction, samples were taken at various times during the photolysis. Samples were obtained by withdrawing 5 mL of reaction solution and passing it through a 0.2 μm filter supplied by Membrane Solutions to remove the solid titanium catalyst. The concentration of organic carbon present in the reaction was then determined using a Shimadzu 5000-TOC Analyzer.

Photocatalytic degradations of p-anisylneopentanol[21] were run using the following method. A slurry with a catalyst concentration of approximately 1 g L^{-1} was prepared by dispersing 100 mg of catalyst into 75 mL pH 8.5 water (3 μM NaOH solution). After 10 minutes of sonication, 20 mL of 1.4 mM *p*-anisylneopentanol stock solution were added in darkness and the pH was adjusted to pH 8.5. After a 30 minute equilibration period oxygen purging was begun. The reaction mixture was allowed to purge for 15 min prior to beginning the photolysis and throughout the photolysis. The pH was manually maintained throughout the reaction.

To track the loss of AN without identifying products, 1 mL samples were removed from the reaction vessel via a needle. The samples were then acidified using Amberlight, centrifuged, and passed through a 0.2 μm filter prior to being run on the HP 1050 HPLC. For product studies, the reaction mixture was acidified with Amberlight. It was then centrifuged and filtered twice with a 0.2 μm before 50.00 mL were collected and concentrated to ~3 mL under reduced pressure. The sample was then flash frozen and lyophilized or extracted with ethyl ether that was then allowed to evaporate in a fume hood. The remaining solid was dissolved in methanol using dodecane as an internal standard and run on an HP 5890 Series

www.manaraa.com

II GC equipped with a 30 m Rtx-5 column and FID detector for analysis. Identification and quantification was achieved by comparison to authentic samples.

Degradations of PAA were performed in a similar manner to the other degradations with 50 mg of catalyst being suspeneded in 37 mL DI and sonicated for 10 minutes. 13 mL of 0.6 mM stock solution of phenyl acetic acid was then added to give a final concentration of ~0.15 mM. The mixture was allowed to stir in the absence of light for 30 minutes prior to the addition of oxygen 15 minutes before the start of photolysis. At appropriate intervals 1 mL samples were removed and filtered through a 0.2 μm filter. The samples were then run on the HP 1050 HPLC with an eluent system of 1:1 methanol : water with 0.5% acetic acid and a flow rate of 0.9 mL min^{-1}. Products were identified by comparison to authentic samples and quantified by the response they invoked from the detector. All photolysis were performed at natural pH.

2.4 RESULTS AND DISCUSSION

For ease of discussion all catalysts will be named using the following procedure. Iodine modified catalysts will have the prefix I while unmodified ones will have Ti. The temperature at which they were annealed will follow and finally an N will be added if they were annealed under nitrogen. If no letter follows, they were annealed in air.

Catalyst Characterization

As can be seen in Figure 1, increased annealing temperature led to a larger red shift, resulting in a vivid yellow color for the catalyst annealed at 400 ˚C, which darkened to a tan color as the annealing temperature was increased to 600 ˚C. Though the catalysts annealed at 600 ˚C do have a long tail, which is responsible for its tan color, the more important feature is the initial red shift of the frontier that can be seen at shorter wavelengths. The annealing atmosphere did not have a significant effect; the color of the catalysts was consistent regardless of annealing atmosphere. This is reflected in the UV/Vis spectra of the catalysts annealed at the same temperature but under different atmospheres are very similar.

www.manaraa.com

Figure 1. Diffuse reflectance spectra (DRS) of unmodified anatase TiO_2, the modified catalyst prior to annealing, and ITi 400 and ITi 600.

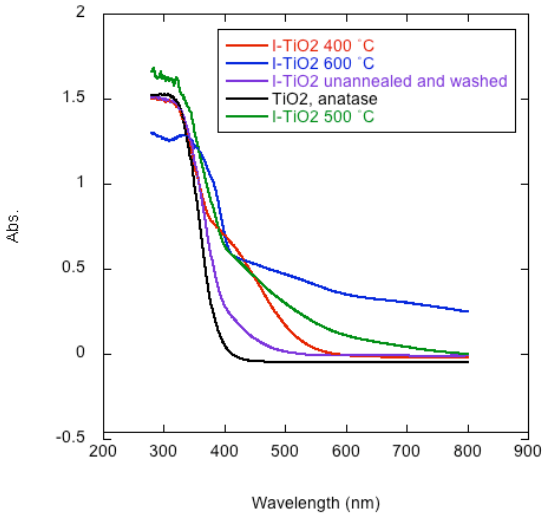

The XP spectra showed that iodine was present in the same oxidation states for catalysts annealed at the same temperature regardless of annealing atmosphere, except in the case of ITi 600 N, which contained amounts of iodine below the detection limit of the instrument. See Table 1 for the amounts of iodine present in each catalyst. As in the previous study, varying the annealing temperature altered the oxidation state of the iodine in the catalysts.[5] XP spectra taken of the catalysts show that the catalysts annealed at lower temperatures have a higher oxidized species of iodine present. When tracking the I_{3d5} peak, ITi 600's is located at 618.9 eV which has been ascribed to I^- [19,23-25] while catalysts annealed at 400 °C have the I_{3d5} peak at 624.5 eV which has been reported to be either I^{5+} [5,23,26] or I^{7+} [24-26]. In either case, the point remains that lower temperatures yield higher oxidation states. The catalysts annealed at 500 °C have a mixture of oxidation states containing both I^- and the disputed I^{5+}/I^{7+}.

www.manaraa.com

Table 1. Percentages of iodine present in each catalyst.

Temperature	Annealed Under Air	Annealed Under N_2
400	3.14	2.85
500	0.16	0.14
600	0.34	-

Though it may be thought that a non-oxidizing atmosphere may lower the oxidation states of the iodine in the catalyst, this was not observed. The fact that ITi 600 was found to contain a measurable amount of iodine while ITi 600 N does not contain iodine may have more to do with the way the catalysts were annealed rather than the annealing environment. During the annealing process, a constant, though slow, stream of nitrogen was passed over the catalysts, which may have increased the rate of iodine loss by blowing off vaporized iodine. Under air, the system was open but stagnant.

The most interesting point that can be taken from this is ITi 600 N looks the same as ITi 600 and *generally behaves similarly* even though it lacks dopant. It is unclear why ITi 500 had less iodine than ITi 600 incorporated into its lattice.

www.manaraa.com

Figure 2. XPS spectra of the catalysts. Catalysts annealed under air are in the top row and catalysts annealed under nitrogen are in the bottom row. All of the graphs are plotted C/S vs. Binding Energy (eV).

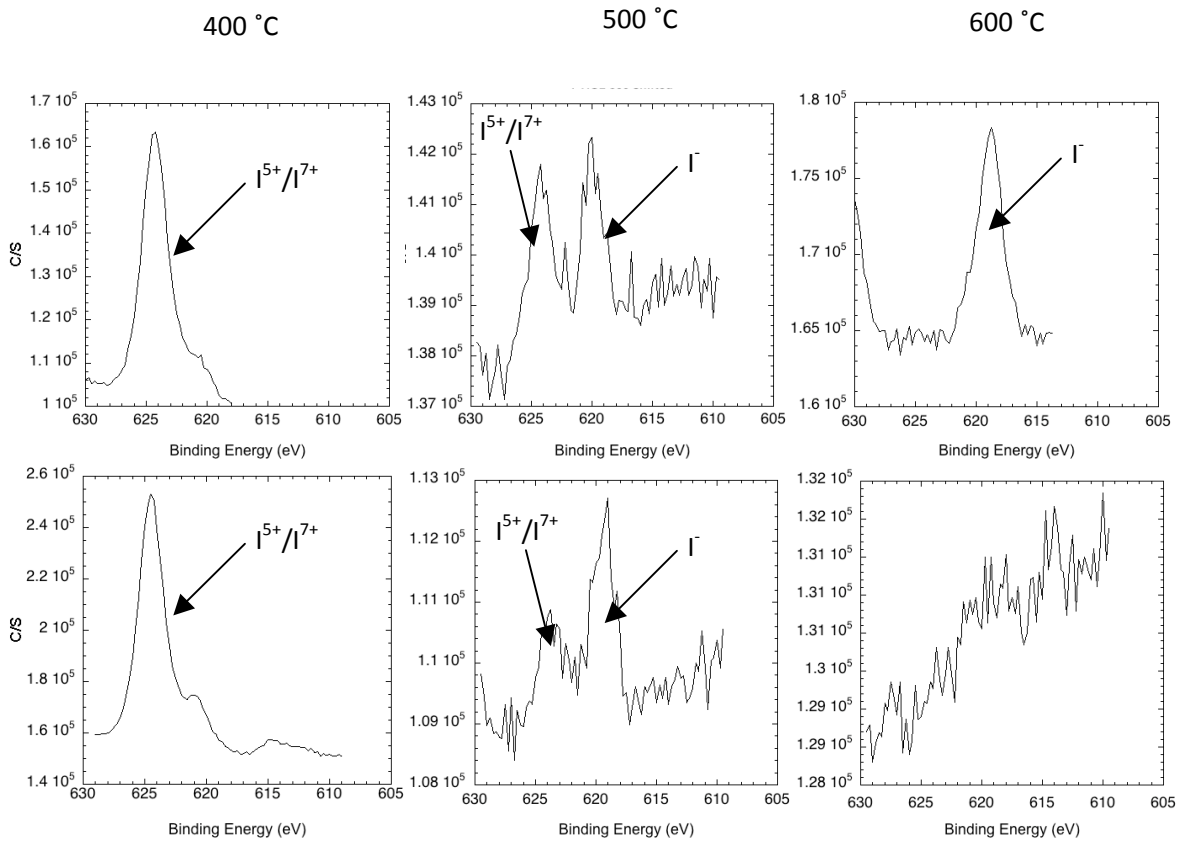

One explanation as to why ITi 600 N and ITi 600 both appear and behave similarly is based on the argument that oxygen deficiencies, and not band gap narrowing or the introduction of midgap states by dopants, are responsible for visible light absorption and reactivity of TiO_2 photocatalysts.[27-29] Thompson *et al.* showed that annealing at temperatures from 600 K (327 ˚C) to 900 K (627 ˚C) lead to increasing amounts of oxygen vacancies present in the catalyst.[29] Since 600 ˚C is close to the optimum temperature for oxygen vacancy formation, it follows that ITi 600 (N) have greater absorbance in the visible region relative to the other catalysts. However, the fact that unmodified TiO_2 600 does not look or necessarily act like ITi 600 N implies that the dopant has some effect on formation of the catalyst. The most probable explanation is that the iodine dopant initially stabilizes defects and encouraged their formation. I^- should substitute for O^{2-} , because I will only replace

www.manaraa.com

titanium if it is I^{5+}.[30] When I^- substitutes for O^{2-}, Ti^{4+} would have to be replaced by Ti^{3+} to maintain bulk charge neutrality. After this, it burnt off introducing more defects. Dopants have been shown to stabilize Ti^{3+} defects,[27] and this may account for some of the differences seen in the reactivity of ITi 600 and ITi 600 N as this stabilizing effect can still exist in ITi 600 but not ITi 600 N.

Yang, *et al*. suggested that any iodine doped catalyst would have a decrease in its band gap of 0.6 eV,[30] however this should mean that all of the catalysts would have the same color, yellow. We found however that higher annealing temperature increased visible light absorption, for all of the modified catalysts including ITi 600 N, which contains no iodine. This implies that it is solely oxygen vacancies that are responsible for visible light absorption.

It could actually be expected that ITi 500 (N) would have the most defects as it has not only I^-, which could induce defect formation as previously discussed, but also more oxidized iodine species which would give the bulk crystal a large positive charge if Ti^{4+} were not to convert to Ti^{3+}. Though this could help explain why ITi 500 (N) is the most visible light active, it does not fully explain why it does not absorb as much visible light at ITi 600 (N). ITi 400 (N)'s defects would likely stem from the conversion Ti^{4+} conversion to Ti^{3+} to offset the larger positive from the I^{5+}/I^{7+} present so that overall neutrality can be maintained. This difference in defect origin may be able to explain the differences in the UV-Vis of the catalysts, mainly the shoulder and tailing differences.

Annealing temperature also had an effect on the surface acidity of the catalysts. Table 2 gives the PZC of each catalyst as calculated by duplicated runs and the value that was obtained by placing the catalyst in deionized water. It also gives the PZC of unmodified catalysts annealed under identical conditions for comparison. The catalysts annealed at lower temperatures are more acidic than those annealed at higher temperatures. It should be noted that for all their similarities, here ITi 600 N more closely resembles Ti 600 than ITi 600. Otherwise, the catalysts annealed under nitrogen are generally more basic than their air annealed counterparts.

www.manaraa.com

Table 2. The point of zero charge for each catalyst found using the potentiometric mass titration technique (PMT) and the pH when the catalyst is added to deionized water.

Catalyst	PMT method	Water
Ti 400	5.00	5.12
I-Ti 400	2.50	2.56
I-Ti 400 N	3.00	2.77
Ti 500	6.00	5.28
I-Ti 500	5.75	3.90
I-Ti 500 N	6.50	3.55
Ti 600	4.50	5.80
I-Ti 600	6.50	5.77
I-Ti 600 N	4.11	3.58

Photocatalytic degradation of quinoline

Quinoline has been found to degrade by both hydroxyl radical ($^{\bullet}OH_{ads}$) and SET chemistry, but depending on the degradation pathway used, different products will be produced as shown in Scheme 1. [20] For this reason, quinoline has become a valuable probe for determining the degradation mechanism that occurs at the surface of catalysts being studied.

The apparent rates, k_{app}, found during photocatalytic degradations of quinoline are shown in Table 3. Due to different light sources and experimental procedures, the rates are only internally comparable, with the exception of the UV pH 3 and pH 6 photolyses. This two may be directly compared.

www.manaraa.com

Table 3. Rates of quinoline lost during degradations (μM/min) under specified conditions over synthesized catalysts.

UV Ar pH3			
	400	**500**	**600**
I-TiO_2 Air	0.36	0.16	0.15
I-TiO_2 N_2	0.35	0.23	0.04
TiO_2	0.05	0.08	0.05
Vis pH6			
	400	**500**	**600**
I-TiO_2 Air	0.02	0.04	0.01
I-TiO_2 N_2	0.03	0.03	0.02
TiO_2	0.01	0.01	0.02
UV pH3			
	400	**500**	**600**
I-TiO_2 Air	0.41	0.13	0.06
I-TiO_2 N_2	0.16	0.21	0.1
TiO_2	0.61	1.1	1.3
UV pH6			
	400	**500**	**600**
I-TiO_2 Air	0.37	0.39	0.17
I-TiO_2 N_2	0.53	0.45	0.28
TiO_2	1.2	1.2	2.8

[a] P25 was found to give a rate of 0.02

As can be seen in Table 2, both the temperature and atmosphere of annealing had some effect on the catalysts' efficiency. Modified catalysts annealed at 600 °C are always slower than the lower annealing temperature catalysts. Under UV irradiation, the unmodified materials are significantly faster than the doped materials when the solution is aerated, and the degradation of quinoline is more efficient at pH 6 than pH 3 for all catalysts with the exception of ITi 400. Catalysts annealed under nitrogen are more efficient than those annealed in air when UV irradiation is employed, with the exception of ITi 400 for which the

www.manaraa.com

opposite is true. It should be observed that when degradations are purged with oxygen ITi 600 N has rates more similar to ITi 600 than TiO_2 600. This suggests that oxygen vacancies and crystal defects are responsible for catalytic behavior during aerated photolyses.

Under hypoxic conditions the iodine containing catalysts are faster than the catalysts that do not contain iodine (TiO_2 and ITi 600 N). This suggests that iodine plays a key role in hypoxic photolysis, likely acting as an electron sink, and at least temporarily limiting charge recombination. This is also implied because ITi 400 (N), which contains iodine with a high oxidation state also has the greatest rate of degradation. ITi 500 (N) has mixed oxidation states so its rate would be expected to be lower than that of ITi 400 (N) while ITi 600 has reduced iodine, suggesting that it should have the lowest rate.

In order to examine the degradation pathways used by the catalysts, product distributions and mass balances were determined. This was accomplished by measuring the concentration of SET products and $^{\bullet}OH_{ads}$ products. Equation 1 and Equation 2 were then used to determine the percent of the products that were SET products and the mass balance, respectively.

$$[SET] / ([SET] + [^{\bullet}OH_{ads}]) \times 100 \qquad (1)$$

$$([SET] + [^{\bullet}OH_{ads}]) / [\text{quinoline lost}] \qquad (2)$$

Table 4 shows the percent of SET products formed and the *mass balances* of the quinoline degradations. Because the unmodified TiO_2 catalysts produced similar product distributions and mass balances, their distributions and mass balances were averaged to supply one reference value.

www.manaraa.com

Table 4. Product distributions and mass balances found during UV and visible light (Vis) photolyses of quinoline over I-TiO_2 catalysts annealed at specified temperatures and atmospheres at specified pH where the mass balance is italicized. TiO_2 results are shown for comparison.

	400	**500**	**600**	**400 N2**	**500 N2**	**600 N2**	**TiO_2**
UV Ar pH3	100, *3*	7, *27*	0.3, *38*[a]	98, *7*	17[a], *22*	0.2, *16*	6, *35*[b]
Vis pH6	100, *10*	53, *0.5*	100, *5*	100, *1*	32, *7*	22[c], *3*	21, *2*
UV pH3	96, *5*	11, *45*	3, *64*	81, *15*	6, *63*	4, *88*[a]	3, *61*
UV pH6	90, *7*	53, *28*	11[a], *27*	100, *10*	37, *13*	20, *36*	33, *45*

[a] <10% error

[b]Degradation performed over Ti 600 has a mass balance of 85%

[c] 21% error

As can be seen in Table 4, the mass balance of ITi 400 is poor. It may be argued that the product distributions may not be completely accurate, as small variations in product concentrations will be greatly exaggerated due to the small amounts in question. However all results were reproducible within a 5% standard deviation.

Several trends can be seen in these results. When discussing product distribution, the catalysts annealed at 400 ˚C produce SET products almost exclusively under UV irradiation, regardless of aeration, while catalysts annealed at 500 ˚C produce far fewer SET products and catalysts annealed at 600 ˚C produce almost solely $^{\bullet}OH_{ads}$ products. One interesting result is that though ITi 600 N degraded Q at a rate comparable to TiO_2 in hypoxic conditions, its product distribution is more similar to that of ITi 600 under the same conditions. As the annealing temperatures increased, the mass balances generally increased when UV light irradiation was used.

One possible explanation for these trends of increasing hydroxylated products as annealing temperature is increased and the low mass balance of ITi 400 may be found in Hong et al.'s work.[5] Once quinoline undergoes $^{\bullet}OH_{ads}$ chemistry, it becomes a kind of phenol analog. Phenol has been shown to degrade quickly over ITi 400 under visible light irradiation by both Hong and ourselves while catalysts annealed at others temperatures do not degrade

www.manaraa.com

phenol efficiently (Table 5). This would lead to increasing mass balances and higher percentages of hydroxylated products as annealing temperature increased because the $^{\bullet}OH_{ads}$ products would build up more.

Table 5. Apparent rates of phenol degradation under visible light irradiation (λ>435 nm) over the specified catalysts.

I-TiO_2 Annealing Temperature	Apparent Rate (μM/min)
400	0.34
500	0.08
600	0.02

When quinoline's primary degradation products were degraded under UV light irradiation, it was found that 2-aminobenzaldehyde degraded in the dark over ITi 600 at pH 6 and ITi 400 at pH 3 and pH 6. The $^{\bullet}OH_{ads}$ products degraded at rates comparable to phenol over ITi 400 at pH 3 and pH 6. Over ITi 600 at pH 6, rapid degradation was also seen. Over ITi 400, some loss of $^{\bullet}OH_{ads}$ products was seen in the dark at both pHs. The rates of degradation are noted in Table 6.

Table 6. Degradation rates (μM/min) of quinoline (Q) and its primary degradation products under UV light irradiation over the specified catalysts. Quinoline's products are 2-aminobenzaldehyde (2AB), 2-quinolinone (2HQ), 4-quinolinone (4HQ), 5-hydroxyquinoline (5HQ), 8-hydroxyquinoline (8HQ)

	2AB	**2HQ**	**4HQ**	**5HQ**	**8HQ**	**Q**
ITi 600 pH 3	0.04	0.04	0.03	0.03	0.04	0.02
ITi 600 pH 6	0.2	0.04	0.01	0.23	0.18	0.01
ITi 400 pH 3	*	0.04	0.05	0.38	0.22	0.02
ITi 400 pH 6	*	0.04	0.05	0.41	0.27	0.02

*Degradation occurred in the dark so little was left when the photolysis was started.

These rates help explain why ITi 600 has a greater mass balance at pH 3 than pH 6. They also suggest that the product distributions are meaningful as ITi 600 degrades $^{\bullet}OH_{ads}$ products efficiently, yet still shows mostly $^{\bullet}OH_{ads}$ products in its product distribution.

www.manaraa.com

ITi 400 (N) and ITi 600 give 100% SET products, while the catalysts annealed at 500 ˚C and ITi 600 N give a mixture of products. Oftentimes, catalysts produce SET products under visible light irradiation.[16,31] This is one of the few time ITi 600 N behaves differently than ITi 600 by not producing solely SET products. In this case, ITi 600 N acts more like the unmodified catalyst by producing a mixture of products even though neither catalyst annealed at 600 ˚C is an efficient visible light photocatalyst, degrading Q no faster than the unmodified catalysts. This suggests that the dopant may play a role in determining which pathway is used to degrade pollutants. ITi 500 (N) are unique in our study in that they are both visible light active and produce a mixture of degradation products. This may mean that they will be better suited at degrading pollutants that are not prone to SET chemistry.

The issue of what role the dopants play in determining the degradation pathway used by the catalyst requires more study as it is ambiguous. It is tempting to claim that the degradation pathway comes from the oxidation state of the catalyst's dopant. Previous studies that showed SET chemistry occurring during visible light photolyses used catalysts with dopants that had positive oxidation states,[16,31] and ITi 400 has a positive oxidation state. This cannot explain however, ITi 600 producing only SET chemistry as it has a -1 oxidation state. It may be that having a mixture of oxidation states and not the oxidation states themselves is the cause for ITi 500 (N) exhibiting mixed pathways as this is the only difference between ITi 500 (N) and the other iodine containing catalysts.

Photocatalytic degradation of formic acid

Because formic acid has been shown to degrade solely through an SET mechanism, it was chosen to further examine I-TiO_2 degradation method.[13] UV degradations of formic acid proceeded at reasonable rates when the starting concentration was 18 mM. Table 7 shows the change in formic acid concentration over length of irradiation for all tested catalysts with comparable starting concentrations.

www.manaraa.com

Table 7. Apparent rates of formic acid loss (millipercent /min)

Annealing temperature	Air Annealed	N_2 Annealed	Unmodified TiO_2
400	0.3	0.3	1.4
500	1.0	1.5	1.8
600	0.0	0.0	2.0

Though no direct comparison of the rates for the formic acid degradations and Q degradations can be made due to an order of magnitude difference in starting concentration and catalyst concentrations, it can be noted that the unmodified materials are still more efficient than the modified ones. Here, ITi 600 was found to lack any photocatalytic abilities, which agrees with Hong's findings.[5] None of the catalysts are more efficient than the unmodified materials. ITi 500 is almost as efficient as the undoped materials. ITi 500 is superior to ITi 400, which is different from the quinoline degradations as it was significantly less likely to degrade quinoline using SET chemistry. Even so, annealing atmosphere had the same effect on the efficiency of the catalyst to degrade formic acid as it did on the Q product distributions. When degrading quinoline, ITi 500 leaned more towards SET products than ITi 500 N did, and ITi 500 is more efficient than ITi 500 N at degrading formic acid. The same is true for ITi 600 N, which was more likely to degrade Q by SET pathways and here is able to degrade formic acid although modestly, while ITi 600 is not.

Formic acid was not degraded efficiently during visible light photolyses. Initially, the visible light photolyses were run using a starting concentration of 18 mM as it was not too large for the UV photolyses. The starting concentration was then lowered to 3 mM because a change in concentration is being looked for. As a specific change in a large number is much less notable than that same change in a small number, it was thought that a lower concentration may show degradation under visible light. This did not work. Finally, the starting concentration was lowered from 3 mM to 0.016 mM. At 0.016 mM however, carbon contamination from the environment became an insurmountable problem. Because no

www.manaraa.com

degradation could be seen at 3 mM starting concentration, it can be concluded that none of the catalysts are highly efficient at degrading formic acid under visible light irradiation.

Photocatalytic degradation of phenylacetic acid (PAA)

To eliminate the extraneous carbon contamination issues that arose during the formic acid degradations, PAA was used as a probe molecule for it should also degrade preferentially via SET chemistry but can be monitored by HPLC. This would allow the separation of any contaminates that may be introduced by the reaction environment from the probe. In this way it was hoped that the starting concentration could be reduced and that the degradation of the molecule could be studied under visible light irradiation. No visible light activity was noted for any of the catalysts, which was surprising as ITi 400 N degraded quinoline under visible light irradiation via SET chemistry. Under UV irradiation, PAA was degraded in a similar manner to formic acid, with ITi 500 being the fastest, ITi 600 showing little degradation while ITi 600 N showed more degradation. All mass balances appeared to be low (3% - 7%), with the only identifiable product being benzaldehyde. The exception was ITi 500 N, which had a mass balance of 24%. Benzaldehyde was still the only product found. Several unresolved peaks were found, but they were not above the noise level. None of the unresolved peaks had distinct UV-Vis spectra to suggest that they were anything other than noise.

Photocatalytic degradation of p-anisylneopentanol

AN was used to examine the catalyst's ability to degrade a poorly binding substrate and to also shed light on the product distributions given by the catalysts without the problem of products degrading faster than the starting material. None of these catalysts have been shown to degrade AN under visible light irradiation. Because ITi 500 (N) degraded Q via $^{\bullet}OH_{ads}$ chemistry under visible light irradiation, it was thought that ITi 500 (N) may be capable of degrading AN. Since AN is a weakly binding substrate, it is more likely to undergo degradation via $^{\bullet}OH_{ads}$ chemistry than SET chemistry.

www.manaraa.com

2.5 CONCLUSION

I-TiO_2 is extremely efficient with only a specific set of probe molecules. With the exception of phenol, it exhibited only modest visible light efficiency if any. I-TiO_2 was successfully synthesized and characterized. By using several probe molecules, we determined that lower annealing temperatures generally lead to a stronger preference for the SET pathway when UV irradiation is used and that higher annealing temperatures lead to increased use of $^{\bullet}OH_{ads}$ pathways regardless of annealing atmosphere. It was found that annealing temperature also has a larger effect on the physical properties of the catalyst than annealing atmosphere as both the UV-Vis and oxidation state of the iodine present in the catalyst varied only with annealing temperature while remaining constant when annealing atmosphere changed.

Though some efficiency was lost during degradations with UV irradiation, ITi 400 N and ITi 500 (N) exhibited modest visible light activity when degrading Q, and more importantly, they did it in different ways; iTi 400 N only reacted via SET while ITi 500 (N) reacted with a mixture of SET and $^{\bullet}OH_{ads}$ which suggests that it may be able to degrade poorly adsorbing pollutants that do not react readily via SET pathways. All of the iodine containing catalysts proved to be highly effective under hypoxic conditions under UV irradiation.

With this study, experimental evidence in support of the theory that the defects caused by the introduction of dopants are responsible for photocatalysts' behavior rather than the dopants themselves has been gained. This is shown by ITi 600 N, which though it contains no iodine, acts in a very similar way to its iodine containing counterpart (ITi 600). This is of great value as it helps us understand the more fundamental workings of photocatalysts. It may be that we are able to use less dopant materials, which could improve cost effectiveness, or that we could synthesize the catalysts in the presence of a dopant that is later removed which could eliminate concerns about toxic dopants leaching out of the catalysts during use.

2.6 ACKNOWLEDGEMENTS

The authors gratefully acknowledge Brian Trewyn for allowing us to obtain DRS spectra on his instrument and Jim Anderegg for his assistance with collecting and interpreting XPS.

www.manaraa.com

2.7 REFERENCES

(1) Hong, X.; Wang, Z.; Cai, W.; Lu, F.; Zhang, J.; Yang, Y.; Ma, N.; Liu, Y. *Chem. Mater.* **2005**, *17*, 1548.

(2) Gaya, U. I. A., A. H. *Journal of Photochemistry and Photobiology C: Photochemistry Reviews* **2008**, *9*, 1.

(3) Fujishima, A.; Zhang, X.; Tryk, D. A. *Surface Science Reports* **2008**, *63*, 515.

(4) Abdullah, M.; Low, G. K.-C.; Matthews, R. W. *J. Phys. Chem.* **1990**, *94*, 6820.

(5) Hong, X. W., Z.; Cai, W.; Lu, F.; Zhang, J.; Yang, Y.; Ma, N.; Liu, Y. *Chem. Mater.* **2005**, *17*, 1548.

(6) Long, R.; English, N. J. *J. Phys. Chem. C* **2009**, *113*, 9423.

(7) Grassian, V. H. In *Environmental Catalysis*; CRC Taylor & Francis: Boca Raton, 2005, p 307.

(8) Pichat, P. *Water Science & Technology* **2007**, *55*, 167.

(9) Serpone, N.; Lawless, D.; Disdier, J.; Herrmann, J.-M. *Langmuir* **1994**, *10*, 643.

(10) Rockafellow, E. M.; Stewart, L. K.; Jenks, W. S. *Applied Catalysis B: Environmental* **2009**, *91*, 554.

(11) Cermenati, L.; Pichat, P.; Guillard, C.; Albini, A. *J. Phys. Chem. B* **1997**, *101*, 2650.

(12) Hathway, T.; Jenks, W. S. *Journal of Photochemistry and Photobiology A: Chemistry* **2008**, *200*, 216.

(13) Bernardini, C. C., G.; Dozzi, M. V.; Selli, E. *Journal of Photochemistry and Photobiology A: Chemistry* **2010**.

(14) Maki, Y.; Sako, M.; Oyabu, I.; Murase, T.; Kitade, Y.; Hirota, K. *J. Chem. Soc, Chem. Commun.* **1989**, 1780.

(15) Ranchella, M. R., C.; Sebastiani, G. V. *j. Chem. Soc., Perkin Trans. 2* **2000**, 311.

(16) Rockafellow, E. M.; Stewart, L. K.; Jenks, W. S. *Applied Catalysis B: Environmental* **2009**, *91*, 554.

www.manaraa.com

(17) Ohno, T. M., T.; Matsumura, M. *Chem. Lett.* **2003**, *32*, 364.

(18) Ohno, T. t., T.; Toyofuku, M.; Inaba, R. *Catal. Lett.* **2004**, *98*, 255.

(19) Vakros, J. K., C.; Lycourghiotis, A. *Chem. Commun.* **2002**, 1980.

(20) Cermenati, L. P., P.; Guillard, C.; Albini, A. *J. Phys. Chem. B* **1997**, *101*, 2650.

(21) Rockafellow, E. M. S., L. K.; Jenks, W. S. *Applied Catalysis B: Environmental* **2009**, *91*, 554.

(22) Abdullah, M. L., L.; Matthews, R. W. *J. Phys. Chem.* **1990**, *94*, 6820.

(23) Song, S. T., J.; Xu, L.; Xu, X.; He, Z.; Qiu, J.; Ni, J.; Chen, J. *Chemosphere* **2008**, *73*, 1401.

(24) Su, W. Z., Y.; Li, Z.; Wu, L.; Wang, X.; Li, J.; Fu, X. *Langmuir* **2008**, *24*, 3422.

(25) Tojo, S. T., T.; Fujitsuka, M.; Majima, T. *J. Phys. Chem. C* **2008**, *112*, 14948.

(26) Liu, G. C., Z.; Dong, C.; Zhao, Y.; Li, F.; Lu, G.Q.; Cheng, H. *J. Phys. Chem. B* **2006**, *110*, 20823.

(27) Emeline, A. V.; Sheremetyeva, N. V.; Khomchenko, N. V.; Ryabchuk, V. K.; Serpone, N. *The Journal of Physical Chemistry C* **2007**, *111*, 11456.

(28) Kuznetsov, V. N.; Serpone, N. *J. Phys. Chem. B* **2006**, *110*, 25203.

(29) Thompson, T.; Yates, J. *Topics in Catalysis* **2005**, *35*, 197.

(30) Yang, K.; Dai, Y.; Huang, B.; Whangbo, M.-H. *Chemistry of Materials* **2008**, *20*, 6528.

(31) Rockafellow, E. M.; Haywood, J. M.; Witte, T.; Houk, R. S.; Jenks, W. S. *Langmuir* **2010**, *26*, 19052.

www.manaraa.com

Chapter 3. Limitations of bismuth oxyiodide in photodegradations

Deborah R. Lipman Chernyshov, Gregory Thompson, and William S. Jenks

Department of Chemistry, Iowa State University, Ames, IA 50011-3111, United States

This is a draft of a paper that will be published once a few final experiments are completed. The author of this thesis is responsible for the synthesis of the catalysts and most of the kinetic data. The author is grateful to Gregory Thompson who performed the point of zero charge experiments and assisted with some photolyses.

3.1 ABSTRACT

Bismuth oxychloride (BiOCl), bismuth oxybromide (BiOBr), and bismuth oxyiodide (BiOI) catalysts were prepared using the sol-gel method. All of the BiOX (X= Cl, Br, I) catalysts exhibited significant activity when degrading phenol. BiOI however, lacked the ability to degrade any other probe molecules (*p*-anisylneopentanol, phenylacetic acid, and quinoline) efficiently under UV or visible light irradiation. BiOBr and BiOCl both degraded quinoline significantly slower than they did phenol under UV irradiation. These finding suggest that phenol is easily degraded by some mechanism that is not yet fully understood, and that these catalysts exhibit high efficiency with only a select group of probe molecules.

3.2 INTRODUCTION

To date, TiO_2 has been the focus of many studies as a potential photocatalyst for pollutant remediation. Due to its inability to absorb visible light, it is not efficient and while many attempts to improve its visible light absorption have been made, only modest improvements have been realized.[1] The difficulties encountered while trying to improve TiO_2 have lead researchers to look for other semiconductors that exhibit photocatalytic abilities under visible light irradiation.

One of the more promising candidates is the family of bismuth oxyhalides, in particular bismuth oxyiodide (BiOI), as it has been shown to degrade a variety of pollutants under

www.manaraa.com

visible light and simulated solar irradiation.[1-3] Though its potential as a photoctalyst has been demonstrated by degrading a select group of probe molecules,[4,5] little is know about how it degrades pollutants or how large a variety of pollutants it can degrade. In this study we synthesized BiOI and using a diognostic series of probe molecules, determined what structural characteristics a probe must have to be degraded by BiOI efficiently.

3.3 EXPERIMENTAL

Materials

All chemicals were purchased at reagent grade or higher and used without further modifications. The water used in all experimental procedures was purified using a Milli-Q UV plus system and was found to have a resistance of 14.5 MΩ/cm or higher. *p*-Anisylneopentanol (AN) was prepared using literature methods.[6]

Catalyst Preparation

The catalysts were prepared using modified versions of previously reported synthetic methods. Method A,[1] required that 4.85 g bismuth(III)nitrate pentahydrate ($Bi(NO_3)_3•5H_2O$) be dissolved in 7 mL of acetic acid. This solution was then quickly added to a 100 mL aqueous solution containing 1.5 g sodium iodide and 1.64 g sodium acetate. The resulting mixture was then sealed and stirred for approximately 24 hours, prior to collecting the precipitated catalyst and washing it 3 times with DI. The catalyst was dried in a 70 ˚C oven prior to further use or annealing. This sample has been denoted as BiOI A.

In Method B[2], 10 g $Bi(NO_3)_3•5H_2O$ was dissolved in 600 mL 200 proof ethanol prior to the dropwise addition of 4 g KI dissolved in 600 mL DI. After the addition was complete, the mixture was allowed to stir overnight. The precipitate was then collected, washed with 200 proof ethanol once and deionized water twice. The catalyst was then dried overnight in a 70 ˚C oven prior to use or annealing and will be referred to as BiOI B.

Method C[1] (BiOI C) was a large scale version of Method A, but was produced in a slightly more acidic environment, resulting in a slightly paler colored catalyst. 24 g of $Bi(NO_3)_3•5H_2O$ were dissolved in 50 mL acetic acid. This was then added quickly to a 500 mL aquesous solution containing 5.25 g sodium iodide and 8.2 g sodium acetate.

www.manaraa.com

Bismuth oxychloride (BiOCl) and bismuth oxybromide (BiOBr) were synthesized for comparison using Method A. Instead of using sodium iodide however, sodium chloride or potassium bromide were used.

Photocatalytic Ability

Photocatalytic ability was tested through degradations of several probe molecules, quinoline, *p*-anisylneopentanol, and phenylacetic acid. All visible light degradations were performed using a Xenon arc lamp equipped with a 435 nm long pass filter. To regulate the temperature of the samples, a water IR filter and 2 electric fans were employed. The light source for all UV degradations was a minirayonet reactor equipped with 8 x 350 nm broad range 4 W bulbs as a light source. The resulting samples were analyzed using two HPLCs. A Varian Prostar equipped with a C18 column and photodiode array detector was used to analyze product distributions and an HP 1050 equipped with a C18 column and photodiode array detector was used to collect kinetic data except, where otherwise stated.

Prior to all photolyses, the reaction mixtures were permitted to equilibrate in the dark for a total of 45 minutes. During the last 15 minutes of equilibration oxygen purging was begun and continued throughout the reaction unless otherwise stated.

Several probe molecules were employed to study the catalyst's reactivity. Phenol is known to be degraded rapidly by BiOI so it was degraded as a positive control.[7] For this control, 0.2 mM solutions of phenol were degraded over the catalysts. The catalyst concentration was 1 mg mL^{-1} with a total reaction volume of 100 mL. At appropriate times, a 6 mL portion was removed via syringe and filtered through a 0.2 mm syringe filter. The solution was then added to a quartz cuvette and the absorption at 270 nm was monitored on an UV/Vis spectrophotometer to quantify the loss of phenol.

Quinoline (Q) degradations were performed using 0.15 mM solutions of Q and catalyst concentration of 1.1 mg mL^{-1}. The pH was maintained at pH 3 ± 0.5 or 6 ± 0.5 using nitric acid and sodium hydroxide. During the photolysis no more than 1 mL of acid and base was added so as to not alter the probe concentration too greatly. Some degradations were performed at natural pH, with no pH adjustment. At selected times ~1.5 mL of solution was removed from the reaction vessel via needle and syringe. 1.00 mL was then taken and acidified with 10 μL of 1 N sulfuric acid prior to centrifuging and filtering through a 0.2 μm

www.manaraa.com

syringe filter. Kinetic data was then collected on the HP 1050 HPLC previously described. An elluent of 75:25 water (0.2% acetic acid) : methanol was used with a flow rate of 0.9 mL min^{-1}.

Co-degradations of quinoline and phenol were performed using a catalyst concentration of 1 mg mL^{-1}, 0.11 mM phenol, and 0.12 mM quinoline with a total volume of 100 mL. The pH was adjusted with sodium hydroxide or nitric acid as needed to maintain pH 6 +/- 0.5. Samples were taken and treated using the same method as quinoline samples. The kinetics of quinoline were determined using the previously discussed HPLC technique. To monitor the loss of phenol, the samples were also analyzed using the HP 1050 HPLC with an eluent of 1:1 water (0.5% acetic acid) and methanol and a flow rate of 0.6 mL min^{-1}.

p-Anisylneopentanol (AN) was degraded using a catalyst concentration of 1 mg mL^{-1} and probe concentration of 0.2 mM. At various times ~1 mL of sample was withdrawn via syringe and needle, acidified with Amberlight, centrifuged and filtered through a 0.2 μm syringe filter prior to being run on the HP 1050 HPLC. The HPLC runs were performed with a 70:30 acetonitrile and water (0.2% acetic acid) eluent and flow rate of 1.0 mL min^{-1}.

Phenylacetic acid (PAA) degradations were performed using a catalyst concentration of 1 mg mL^{-1} and probe concentration of 0.16 mM with a total volume of 50 mL. At given time intervals, ~1 mL of solution was removed and filtered through a 0.2 μm syringe filter prior to analysis on the HP 1050 HPLC. For analysis, an eluent of 1:1 water (0.5% acetic acid) and methanol and a flow rate of 0.9 mL min^{-1} was used.

UV/Vis spectra were obtained using a UV/Vis spectrometer that was equipped with a diffuse reflectance accessory using barium sulfate as a background.

3.4 RESULTS AND DISCUSSION

Catalyst Preparation and Characterization

Through visual analysis, it was apparent that the catalysts had different colors; see Figure 1. This was consistent with the differences among their UV/Vis spectra obtained by diffuse reflectance spectroscopy (DRS) as shown in Figure 2. BiOCl absorbs no visible light; it appears white. BiOBr absorbs some visible light, accounting for its pale yellow color, and BiOI absorbs far into the visible region, accounting for its shades of red-orange as shown in

www.manaraa.com

Figure 1. Though all of the BiOI catalysts had the same absorption onset, how much of each wave length they absorb begins to vary around 650 nm, which reflects their slight variations in coloring. It was originally thought that the color variation could signify some catalytic differences so all the samples were tested for photocatalytic efficiency, but no significant differences were found after degrading phenol, AN, Q, and PAA. The catalysts will therefore not be distinguished from each other from this point on.

www.manaraa.com

Figure 1. Photographs of the synthesized catalysts: a) BiOI - in order from upper left to lower right, BiOI: D, A, B, and C; b) BiOBr c) BiOCl

a.

b.

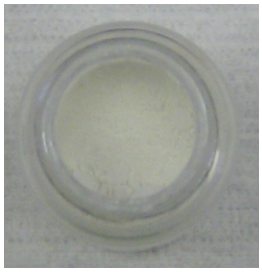

c.

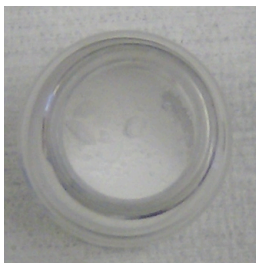

www.manaraa.com

Figure 2. UV/Vis spectra of the synthesized catalysts. Note that absorbance above 1 is considered complete so the variations above 1 are of no significance.

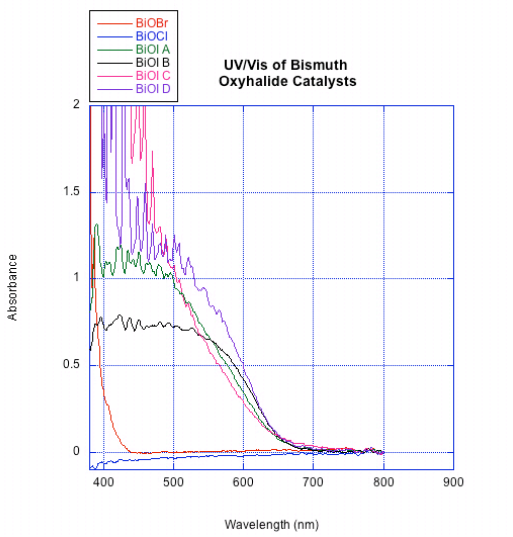

Photocatalytic Ability of BiOI

The BiOI catalyst showed high visible light activity and degraded phenol readily under both visible and UV light. However, when quinoline was used as a probe molecule, little degradation was seen under either light source. It has been suggested that the BiOI degrades pollutants through SET mechanisms,[3] which requires adsorption of the substrate to the catalyst. Quinoline binds differently depending on the pH of the solution due to its pKa of 4.85[8]. Figure 3 shows quinoline and its conjugate acid, the quinolinium ion. For this reason pH 3 and pH 6 were tested. Quinoline was also degraded with no adjustment of pH; the solution's pH was approximately pH 5. This was done to ensure that counter ions of the base/acid could not interfere with quinoline's adsorption.[9] All of these conditions resulted in an inefficient rate of quinoline loss. A thermal degradation of phenol was attempted by warming it to approximately 30 ˚C in the presence of the catalyst to see if the slight warming that occurred due to the light source was a contributing factor to its rapid degradation, but no thermal degradation occurred.

www.manaraa.com

Figure 3. Structure of quinoline and its conjugate acid.

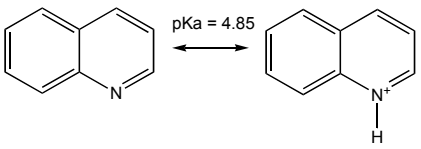

To confirm that the lack of degradation was due to the catalyst's inability to degrade quinoline and was not an artifact of some other variation not already ruled-out, BiOI was used in a co-degradation of Q and phenol. While almost 60% of the phenol was removed over the course of approximately 2.5 hours, no quinoline was lost. Because quinoline and phenol contain aromatic rings and atoms that have lone pair electrons so it would be expected that they should have similar binding patterns. Quinoline is also known to undergo SET chemistry so an inability to be degraded in that manner is not of concern.[10,11] BiOI's inability to degrade quinoline effectively suggests that the catalyst, though impressively efficient with certain probes, may lack the robustness needed for general pollutant remediation.

Other probe molecules were tested to see what structural requirements were necessary for the catalysts to exhibit their high efficiency. AN was degraded to determine if its structural similarities to phenol would elicit rapid degradation by the BiOI catalysts. Though it is known to be a poorly binding substrate,[12] which would not encourage SET reactions, the degradation pathway most literature sources believe to be used by the catalysts, it similar to phenol in structure with regards to the presence of an alcohol group. It is true that containing a methoxy group means it less likely to bind than if the methoxy was a hydroxy group as it is in phenol,[13] but it is still closer in structure to phenol than quinoline so it was hoped that it would degrade more efficiently.

AN was found to degrade at a similar rate to quinoline, which is interesting. If it is assumed that the rapid rate of phenol degradation is due to superb binding and SET chemistry, it would make sense that AN would degrade less quickly than phenol as it adsorbs less effectively than phenol, but it would also be expected that it would bind more than quinoline due to its similarities in structure with phenol thereby degrading faster than quinoline. Because this is not observed, it suggests that the lack of degradation may be due more in part to the catalyst's inability to oxidize the probes rather than adsorption issues. It

www.manaraa.com

may also indicate that phenol undergoes some other degradation pathway beyond standard SET and hydroxyl chemistry, which as of yet is not understood.

To confirm that adsorption was not the reason for poor catalytic performance, phenylacetic acid was used as because it is expected to be a strongly binding substrate at low pH and undergoes SET reaction readily.[14-16] Even so, PAA was found to not degrade significantly faster than AN or quinoline when it was degraded at pH 4. This appears to confirm that BiOI, though very efficient with particular probes, lacks the robustness necessary for pollution remediation.

Because quinoline was not degraded efficiently even when codegradations were performed using UV light, it was wondered if the problem was strictly BiOI's oxidative ability. To eliminate this option, codegradations of phenol and Q were performed over BiOBr and BiOCl under UV light irradiation as these are known to have valance bands with more positive redox potentials than BiOI. BiOI's valance band lies at 2.32 eV while BiOBr and BiOCl's valance bands lie at 3.19 eV and 3.65 eV respectively (See Figure 4).[3,17-20] The goal of these experiments was to see if Q was degraded as quickly as phenol was by these catalysts, as this would suggest that it is the oxidative ability of BiOI that leads to its inefficiency. If however the same pattern of phenol being degraded far faster than Q was found, it would suggest that there is something unique about phenol, either in its ability to adsorb to the catalysts or some degradation mechanism that it undergoes that is not understood at this time. The later was found to be true as though BiOBr and BiOCl both degraded quinoline more rapidly than BiOI did under the same conditions, they did not degrade both quinoline and phenol at comparable rates. From this we can conclude that though oxidative ability likely plays some part in BiOI's inability to degrade quinoline effectively, this is not the sole factor. Due to the variety of probes that BiOI has trouble degrading effectively, it appears that phenol may be a special case that degrades easily through some pathway that is not yet fully understood.

www.manaraa.com

Figure 4. Schematic drawing of BiOX (X= Cl, Br, I) valance band and conduction band

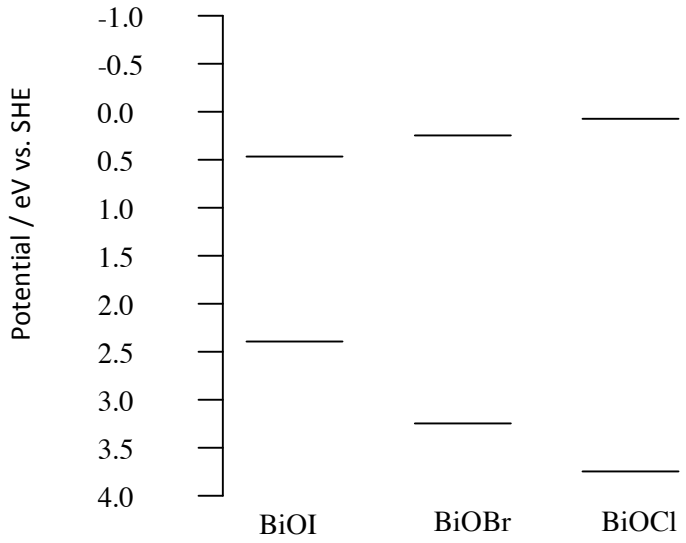

3.5 CONCLUSIONS

Bismuth oxyiodide, bismuth oxybromide, and bismuth oxychloride were successfully synthesized using modified literature methods showing that they are reproducible.[1,2] Slight variations in the synthetic method caused color variations amongst the BiOI catalysts, but appeared to have no significant effect on their catalytic ability. Though BiOI was highly efficient at degrading phenol under visible light irradiation, it failed to degrade a variety of other probes. It is unclear at present which features promote rapid degradation as AN, a poorly binding probe with similar functionality to phenol, degraded at similar rates to PAA, a strongly binding probe. This unfortunately suggests that though BiOI may be an excellent catalyst for niche applications, it will not be useful as a general catalyst for pollutant remediation in its present state. Further studies are needed to determine what exact characteristics encourage rapid degradation by BiOI so that its full potential in niche applications may be taken advantage of and to determine why phenol is so easily degraded by the catalysts.

www.manaraa.com

3.6 ACKNOWLEDGMENTS

The author would like to thank Brian Trewyn for allowing us to obtain DRS spectra on his instrument.

3.7 REFERENCES

(1) Yu, C.; Fan, C.; Yu, J. C.; Zhou, W.; Yang, K. *Mater. Res. Bull.* **2011**, *46*, 140.

(2) Lei, Y.; Wang, G.; Song, S.; Fan, W.; Pang, M.; Tang, J.; Zhang, H. *Dalton Trans.* **2010**, *39*, 3273.

(3) Chang, X.; Huang, J.; Tan, Q.; Wang, M.; Ji, G.; Deng, S.; Yu, G. *Catalysis Communications* **2009**, *10*, 1957.

(4) Chang, X.; Huang, J.; Cheng, C.; Sui, Q.; Sha, W.; Ji, G.; Deng, S.; Yu, G. *Catalysis Communications* **2010**, *11*, 460.

(5) Zhang, X.; Zhang, L. *The Journal of Physical Chemistry C* **2010**, *114*, 18198.

(6) Ranchella, M. R., C.; Sebastiani, G. V. *j. Chem. Soc., Perkin Trans. 2* **2000**, 311.

(7) Li, Y.; Wang, J.; Yao, H.; Dang, L.; Li, Z. *Journal of Molecular Catalysis A: Chemical* **2011**, *334*, 116.

(8) Hosmane, R.; Liebman, J. *Structural Chemistry* **2009**, *20*, 693.

(9) Abdullah, M. L., L.; Matthews, R. W. *J. Phys. Chem.* **1990**, *94*, 6820.

(10) Rockafellow, E. M.; Stewart, L. K.; Jenks, W. S. *Applied Catalysis B: Environmental* **2009**, *91*, 554.

(11) Cermenati, L. P., P.; Guillard, C.; Albini, A. *J. Phys. Chem. B* **1997**, *101*, 2650.

(12) Hathway, T.; Jenks, W. S. *Journal of Photochemistry and Photobiology A: Chemistry* **2008**, *200*, 216.

(13) Li, X.; Cubbage, J. W.; Jenks, W. S. *Journal of Photochemistry and Photobiology A: Chemistry* **2001**, *143*, 69.

(14) Bernardini, C. C., G.; Dozzi, M. V.; Selli, E. *Journal of Photochemistry and Photobiology A: Chemistry* **2010**.

www.manaraa.com

(15) Maki, Y.; Sako, M.; Oyabu, I.; Murase, T.; Kitade, Y.; Hirota, K. *J. Chem. Soc, Chem. Commun*. **1989**, 1780.

(16) Oh, Y.-C.; Li, X.; Cubbage, J. W.; Jenks, W. S. *Applied Catalysis B: Environmental* **2004**, *54*, 105.

(17) Wang, W.; Huang, F.; Lin, X. *Scr. Mater*. **2007**, *56*, 669.

(18) Shamaila, S.; Sajjad, A. K. L.; Chen, F.; Zhang, J. *Journal of Colloid and Interface Science* **2011**, *356*, 465.

(19) Jiang, Z.; Yang, F.; Yang, G.; Kong, L.; Jones, M. O.; Xiao, T.; Edwards, P. P. *Journal of Photochemistry and Photobiology A: Chemistry* **2010**, *212*, 8.

(20) Zhang, X.; Zhang, L.; Xie, T.; Wang, D. *J. Phys. Chem. C* **2009**, *113*, 7371.

www.manaraa.com

Chapter 4: Selectivity in the Photo-Fenton and Photocatalytic Hydroxylation of Biphenyl-4-carboxylic Acid and Derivatives (viz. 4-phenysalicylic acid and 5-phenylsalicylic acid)

*Timothy Hathway, Deborah Lipman Chernyshov, and William S. Jenks**

Department of Chemistry, Iowa State University, Ames, IA 50011-3111

This is a modified version of the paper published in The Journal of Physical Organic Chemistry on February 21, 2011 reprinted with the permission of John Wiley and Sons. The author of this thesis is responsible for several of the kinetics and product studies and collected several of the supporting NMR spectra. Timothy Hathway was the primary researcher who synthesized the molecules, collected several NMR spectra and performed many kinetic runs and product studies.

4.1 ABSTRACT

The selectivity of hydroxylation of the distal rings of 4-phenylbenzoic acid, 4-phenylsalicylic acid, and 5-phenylsalicylic acid were determined using partial TiO_2-mediated photocatalytic degradation and photo-Fenton conditions. This separation of the binding site from the phenyl group being hydroxylated allows a less biased evaluation. The hydroxylation regiochemistry behaves as qualitatively expected for an electrophilic reaction, given the assumption that 4-carboxyphenyl is a slightly electron-withdrawing substituent. Selectivity for hydroxylation of the distal phenyl in 4- and 5-phenylsalicylic acid is reversed, due to the reversal of the electronic demand, while adsorption to the TiO_2 surface is assumed to be analogous for the two structures.

4.2 INTRODUCTION

The study of the early oxidation steps of organic molecules under conditions of TiO_2-mediated photocatalytic degradation has been fruitful, at first to understand the chemistry of the mineralization process, and more recently as a probe to explore differences among

www.manaraa.com

catalysts. Broadly, hydroxyl-like chemistry and chemistry driven by single electron transfer (SET) are the two commonly observed modes of reactivity, particularly for aromatic organics.[50-63] Compounds with multiple reactivity modes become useful interrogators of other catalysts; for example we and others have used 4-methoxyresorcinol, quinoline, and 1-anisylneopentanol (1-(4-methoxyphenyl)-2,2-dimethylpropan-1-ol)) as probe molecules[64-68] to evaluate several modified and doped TiO_2 photocatalysts.[69-73]

However, the balance of reactivity is determined not only by functionality, but also by the ability of the molecule to bind to the TiO_2 surface.[59,74-82] We wanted to add to our bank of test molecules, not least because we thought it important to have molecules with different binding modes. Thus the carboxylic acid functionality, common to organic water pollutants and their degradation intermediates was attractive. Here, we describe the partial degradations of biphenylcarboxylic acid derivatives **1**-**3** by TiO_2 and under photo-Fenton conditions used as a control for the hydroxyl-like chemistry.

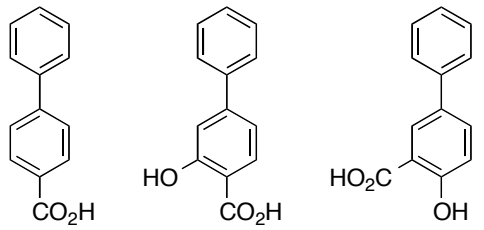

1 **2** **3**

4-Biphenylcarboxylic acid (**1**) was chosen as a starting point for a new probe molecule because it had both the desired functionality and some symmetry that would limit the number of products. We hypothesized that the geometry associated with adsorption through the carboxylate and the differing electron demands of the proximal (di-substituted) and distal (mono-substituted) phenyl moieties might provide a basis for regiochemical selectivity for the SET and hydroxyl-like pathways. We posited that the comparison of **1** to 4-phenylsalicylic acid (**2**) and 5-phenylsalicylic acid (**3**) might prove useful, in that the

www.manaraa.com

additional electron richness of the proximal ring might further enhance SET chemistry. Moreover, to the extent that the relative arrangements of the substituents in **2** and **3** reverse – or at least modify – their electronic influence on the distal phenyl, it was possible that further differentiation might be observed.

A few publications address the regiochemistry of TiO_2-mediated and related hydroxylations, and they broadly suggest that regiochemistry of TiO_2-mediated hydroxylation follows the qualitative rules familiar from standard electrophilic aromatic substitution.[83-89] However, the comparison of substituents necessarily combines the effects of adsorption ability and the electronic effect of the substituent. Compounds **2** and **3** are used to address this question without that ambiguity.

4.3 RESULTS AND DISCUSSION

Partial degradations of **1**, **2**, and **3** were carried out using P25 TiO_2 at pH 8.5 and 12, and also using photo-Fenton conditions at pH 8.5. Solubility limited the ability to run the reactions at low pH, and previous experience had shown that 8.5 is a near-ideal pH for the observation of intermediates in degradations closely related to these.[78,79] At higher pH, the TiO_2 reactions could be done, but the photo-Fenton reactions could not be, due to precipitation of the iron. Three classes of initial reactions were expected under TiO_2 degradation conditions: (a) hydroxylation of the proximal ring, e.g., conversion of **1** to **2**; (b) hydroxylation of the distal ring, e.g., conversion of **1** to **1c** (Chart 1); (c) reactions related to photo-Kolbe decarboxylation through SET at the carboxylate functionality. Previous studies on the degradation of benzoic acid all report formation of salicylic acid, with some reporting observation of other hydroxylated benzoic acids and small amounts of phenol.[90-95]

www.manaraa.com

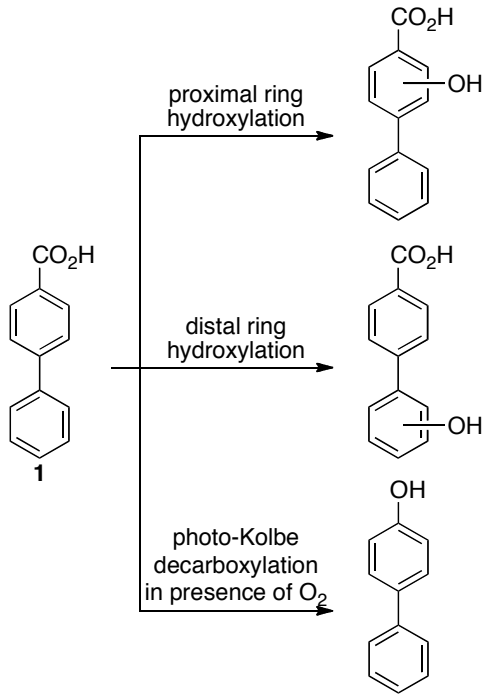

Reasonable zero-order rates were obtained with conversions up to ~25% and are shown in Table 1. (Degradations to higher conversion began to resemble first order decays, as is common for photocatalytic degradations.) All runs were at least duplicated, and error limits in the table represent standard deviations from the average. Control experiments showed that no significant degradation occurred on the timescale of the experiments when the TiO_2 was omitted or if samples were not exposed to light.

www.manaraa.com

Table 1. Initial rates of degradation of **1**, **2**, and **3** using titanium dioxide at pH 12 and 8.5 and the photo-Fenton reaction at pH 8.5

Compound	rate of degradation (μM/min)		
	TiO_2 pH 12	TiO_2 pH 8.5	Photo-Fenton
1	15.1 ± 0.9	13.1 ± 0.7	1.4 ± 0.5
2	15.9 ± 1.0	10.7 ± 0.9	15.3 ± 1.0
3	17.2 ± 1.6	15.6 ± 0.6	14.2 ± 1.4

www.manaraa.com

Chart 1. Starting biphenylcarboxylic acids and their hydroxylated derivatives.

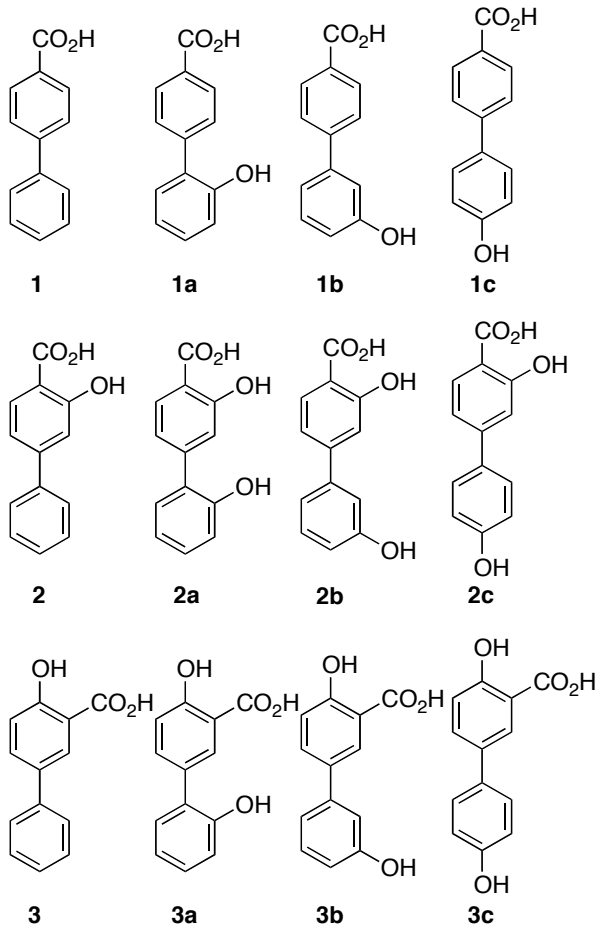

The absolute rate constants, obtained with initial concentrations of 0.25 mM, depend on several experimental parameters, including lamp intensity, sample geometry, etc. However, all physical parameters were held constant for the TiO_2 reactions, so the relative rates are meaningful. Among them, the pH 12 reactions showed no rate variations that could be firmly put outside experimental uncertainties, and the rates at pH 8.5 were all within a factor of about 1.5.

The rates obtained for the photo-Fenton reaction, used as a model for the hydroxyl-type reactivity in TiO_2 chemistry,[52,64,96,97] were coincidentally similar to those obtained for TiO_2 mediated degradations. However, they importantly showed a different internal rate profile,

www.manaraa.com

in that the rate obtained for degradation of **1** was an order of magnitude slower than that for the other two compounds. The simplest explanation for this is that the rates for the TiO_2-mediated reactions are limited by interactions with the TiO_2 surface, while the photo-Fenton reactions revealed rates that reflected more about the inherent reactivity of the compounds.

An alternate and perhaps more probable explanation for the slower removal of **1** under photo-Fenton conditions is based on the hypothesis that the *o*-hydroxycarboxylate functionality tends to chelate iron ions. Thus, compounds **2** and **3** are effectively better ligands for the iron ions than is **1**. As a result, **2** and **3** are degraded faster than **1** because the hydroxyl radicals are formed immediately in their vicinity. Whether truly free hydroxyl radicals are formed at all in Fenton chemistry is a matter of some controversy (See, for example, ref [98].); however, the lack of a free hydroxyl radical would only reinforce this explanation. (The photochemical step of the photo-Fenton reaction is not presumed to be generation of hydroxyl, so the point remains.[99]) Indeed, **1c**, an isomer of **2** and **3** that does not have the *ortho* relationship between its hydroxy and carboxylate functionality, and it was shown (*vide infra*) to degrade at a rate quite similar to **1**, rather than comparable to **2** and **3**.

However, our primary interest was in the product distribution. Three monohydroxylated derivatives of each sharting material were prepared: the products of *ortho*, *meta*, and *para* hydroxylation of the distal phenyl group. They are illustrated in Chart 1 as the "a", "b", and "c" derivatives of each compound, respectively. Compound **2** may be viewed as a hydroxylated derivative of **1**, but no other compounds with hydroxylation of **1**, **2**, or **3** on the ring proximal to the carboxylic acid were prepared. After degradation of 10-20%, samples were exhaustively silylated and examined by GC. Products were identified by their unique retention times (and by co-injection of the authentic samples) on GC and by GC-MS verification of the mass. No singly hydroxylated derivatives of **2** or **3** other than compounds **2a-c** and **3a-c** were observed, i.e., no derivatives of **2** or **3** with hydroxyls on the proximal ring could be detected. (As noted below, **2** was detected as a trace product in degradation of **1**.)

Figure 1 shows the yields of products obtained at 10% conversion of **1**, **2**, and **3** under various conditions. The data are interpolated from multiple runs sampled at various low

www.manaraa.com

percentage conversions to be standardized to the 10% conversion. The relative errors of the yields are ≤ 10%.

Figure 1. Product distributions and mass balance of singly hydroxylated products for degradation of **1**, **2**, and **3** for photo-Fenton reactions and TiO_2 reactions at pH 12 and 8.5 at 10% conversion of starting material. The initial concentration of **1**, **2**, or **3** was 250 μm. The photo-Fenton reactions were carried out at pH 8.5.

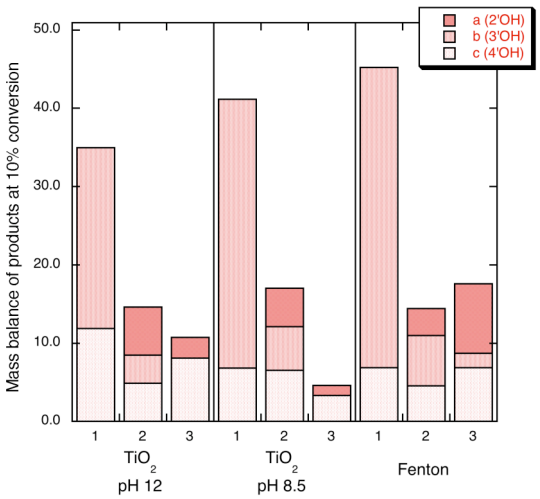

An immediately striking feature of the data in Figure 1 is that the mass balance accounted for by singly hydroxylated compounds for compound **1**, while still below 50%, is significantly greater than that for the other two, under all conditions. Conspicuously missing from all degradations of **1** at low conversion was compound **2**. Also not observed (in any reactions) were biphenyl or 4-phenylphenol.

In the photo-Fenton reactions, at conversions of at least 10%, HPLC analysis of the reaction mixtures revealed many smaller peaks of higher polarity (as judged by chromatography) than any of the compounds in Chart 1. As mentioned previously, the rate of degradation of **1c** was determined under photo-Fenton conditions to see if the degradation rates were correlated simply to the existence of the hydroxyl group. Its degradation rate was 0.8 μM/min, similar to that of **1**. Based on overall electron demand alone, this result is

www.manaraa.com

counterintuitive. It shows that the rate of degradation is sensitive to the relative position of the substituents and is at least consistent with the iron chelation hypothesis to explain the relative rates of degradation of **1**-**3**. Regardless, it became clear that the low overall mass balance was not a hindrance in interpreting the relative product distributions of the distal hydroxylations. Whatever other reactions occur in parallel with the distal hydroxylations, they do not interfere with the relative ratios of the **a**-**c** derivatives among themselves. Analysis at low conversion also ensures that secondary reactions have not grossly disturbed the initial product distributions.

The regioselectivity among the distal hydroxylation products for treatment of **1**, **2**, and **3** can be interpreted using rules of thumb from electrophilic reactions of benzenes. Despite the near-neutral pH, the "4-carboxyphenyl" substituent clearly acts as a slightly electron withdrawing group, favoring the meta-hydroxylation position in the reaction of **1**. The *meta*:*para* selectivity is a little less than 3:1 after accounting for the number of hydrogens (We presume sterics account for the lack of observation of **1a**, but acknowledge that some *ortho* hydroxylation is observed for the other two compounds.) This modest selectivity is consistent with that observed for many weak electron-withdrawing groups for electrophilic reactions of benzene, i.e., it is not the expectation that *meta* functionalization should be the exclusive result.

Given the more rapid initial degradation of molecules **2** and **3** under Fenton conditions, we presume that the qualitative *o*-*m*-*p* distributions are also meaningful. Addition of the 2-OH group to make compound **2** should have the effect of making the phenyl group slightly more electron donating than with the carboxyl group alone, thus somewhat negating its effect as an electron withdrawing group. Indeed, the selectivity for formation of the *meta* product **2b** is quite low. Particularly pleasing from an aesthetic standpoint, however, is the contrast between compounds **2b** and **2c**. By reversing the alignment of the OH and carboxyl groups with compound **3**, the HO group is placed in conjugation to the distal phenyl, presumably greatly increasing its effective electron donation ability to the distal ring. Indeed, although **3b** is still observed, it is clear that the proximal phenyl acts as a mild *o*:*p* director for hydroxylation of the distal phenyl.

www.manaraa.com

TiO_2-mediated hydroxylations

In contrast to the results with the photo-Fenton chemistry, the rates of degradation for compounds **1**, **2**, and **3** were quite comparable to one another, both at pH 8.5 and 12. The simplest explanation for this is that the rate of degradation depends in very large part on the adsorption of the compound to the catalyst, and that this is dominated by the carboxylate functionality, common to all three compounds. Again, a rate check of a representative primary product was performed: **1c** was degraded at 8.4 ± 0.7 μM/min at pH 12, slightly slower than the other compounds.

The hydroxylation product distributions and mass balances obtained for the TiO_2-mediated degradations were qualitatively similar to those obtained with the photo-Fenton reactions, but differed quantitatively in the following ways:

- For **1**, a slightly lower mass balance was obtained, but it was still greater than for the other two compounds. The selectivity for hydroxylation favored the *meta* position still, but to a slightly smaller degree.
- For **2**, the mass balance remained essentially unchanged, but again, somewhat more *ortho* and *para* hydroxylation is observed with TiO_2 than with photo-Fenton.
- For **3**, no *meta* product is observed at all and *para*-hydroxylation predominates to a greater extent over *ortho*.

In other words, the same pattern is observed with respect to *ortho*/*para* vs. *meta* direction using TiO_2 and photo-Fenton, but the overall effect is slightly more biased toward *ortho*/*para* functionalization.

These results are consistent with the notion that the hydroxylation is also taking place with a hydroxyl-like species, but that the adsorption of the carboxylate to the TiO_2 makes it an effectively less electron-withdrawing substituent. Electron transfer mechanisms, i.e., attack of water on, for example, adsorbed $\mathbf{1}^{\bullet+}$, cannot be ruled out, however as water attack on the radical cation results in the same product. (See, for example, refs [100-102] and references contained within, which address the oxidation of phenol.)

www.manaraa.com

Degradations of **1** were carried out to higher conversion (approximately 50%) to try to identify some of the HPLC peaks that (as in the photo-Fenton chemistry) corresponded to downstream oxidation products. Instead of HPLC analysis, the reactions were lyophilized and exhaustively silylated and then subjected to GCMS analysis. In addition to **1b** and **1c**, a trace of **2** was observed, direct evidence of chemistry on the proximal phenyl group. Furthermore, phenylmalonic acid (phenylpropanedioic acid), benzoic acid, and phenol were also observed.

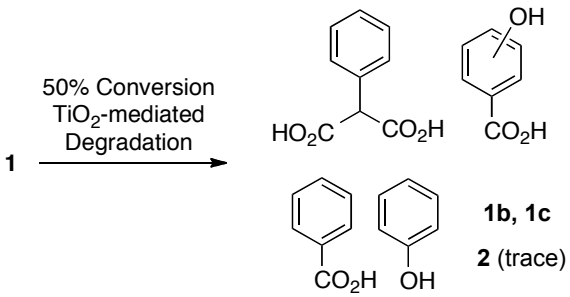

These latter compounds clearly represent multiple steps of degradation, *all* of which occur on the proximal phenyl, or what remains of it. Again, no 4-phenylphenol was observed in previous studies of the degradation of benzoic acid and its hydroxylated derivatives under TiO_2 conditions, up to three hydroxylations of benzene were observed (and extensive ring-opened products were not identified) and phenol was a very minor product at best.[92,103] Nonetheless, these compounds clearly indicate that reactivity can and does occur at the proximal phenyl and that once oxidation begins there, it continues more rapidly than reactivity at the distal phenyl. This is consistent with previous findings[78,79] showing that degradative electron transfer reactions typically become more facile as the ring is oxygenated.

www.manaraa.com

4.4 CONCLUSIONS

Ultimately, it must be concluded that compounds **1-3** are not especially good probes for distinguishing hydroxyl-like chemistry from single-electron transfer chemistry on TiO_2 surfaces. Although it seems clear that there is surface involvement in their primary chemistry (given the nearly identical rates), there is no particular evidence for specific SET-derived products not available through hydroxylation pathways or *vice versa*. The relative dearth of interpretable intermediates low mass balances present another difficulty, in that there is chemistry to which our methods are blind.

Nonetheless, the results reported here surely strengthen the assertion that selectivity in radical-based aromatic hydroxylation under both authentic hydroxyl radical chemistry (photo-Fenton) and TiO_2-mediated conditions can be thought of in terms of a nucleophilic benzene and electrophilic oxidizing agent. Although the biphenyls surely exist with a substantial twist between their π planes, some electronic communication between the rings is expected, and the carboxylic acid acts as a modest electron-withdrawing group. The dramatically different selectivity in hydroxylation of **2** (low selectivity, includes *meta*) and **3** (where the proximal phenyl clearly acts as an *ortho*/*para* director) surely demonstrates a subtlety in selectivity that requires this explanation.

4.5 EXPERIMENTAL

Materials

Compounds **1**, **1c** (Scheme 1), 4-iodobenzoic acid, 4- and 5-iodosalicylic acid, and the phenylboronic acids were used as obtained from commercial sources. Compounds **2** and **3** were prepared via Suzuki-Miyaura coupling using Larock's method,[104] as illustrated in Scheme 1 for compound **3**. The hydroxylated products shown in Chart 1 were prepared in two steps. First, the aldehyde homolog was prepared in the same manner as **2** and **3**; it was then oxidized to the phenol and formic acid under Baeyer-Villiger conditions with *m*-CPBA.[105] Synthetic details are given in the Supporting Information. TiO_2 (Degussa P25) was used as received.

www.manaraa.com

Scheme 1. Suzuki-Miyaura coupling to prepare **3**.

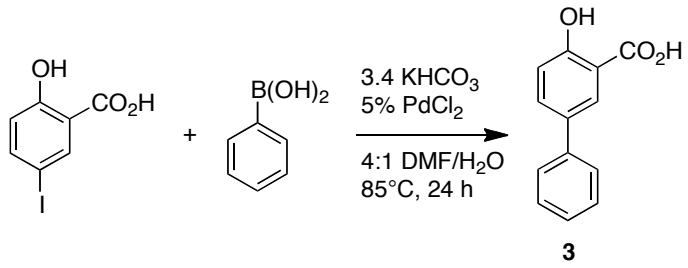

3

Photolyses

The standard suspensions for photocatalytic reactions were prepared to result in 100 mg of TiO_2 per 100 mL of deionized water. To 75 mL of water was added 100 mg of P25 TiO_2. Sonication for five minutes was used to break up larger aggregates of TiO_2. As noted, the pH was adjusted to 12.0 ± 0.5 or 8.5 ± 0.5 by adding 0.1 M NaOH at the start of the reaction and also throughout the reaction as needed to maintain that value. The substrate was added as a 25 mL aliquot from a 1 mM solution of the carboxylate in water to give a final concentration of 250 μm starting material. The mixture was then purged with O_2 and stirred for 30 min in the dark before the irradiation was started. Both stirring and O_2 purging were continued throughout the reaction. Ferrioxalate actinometry[106,107] was used to ensure photon flux remained constant and, in a few instances, to normalize rates to the rest of the data.

Photolyses were carried out with stirring at ambient temperature using a modified Rayonet mini-reactor equipped with a fan and 2 x 4-watt broadly-emitting 350 nm "black light" fluorescent tubes unless otherwise noted. Reaction times were dependent on the degree of degradation required, although 25 minutes was used for kinetic runs.

After appropriate irradiation times, samples were removed and acidified by addition of Amberlite IR-120 ion exchange resin. The TiO_2 and resin were separated by centrifugation, followed by filtration through a syringe-mounted 0.2 μm PES filter. Sample sizes were 1 mL for kinetics or 50 mL for product studies. The latter, larger samples were concentrated by rotary evaporation to approximately 2 mL and the residual water was removed by lyophilization.

www.manaraa.com

For GC-MS product studies, lyophilized 50 mL samples were exhaustively silylated by treatment with 1 mL of anhydrous pyridine, 0.2 mL of 1,1,1,3,3,3-hexamethyldisilazane (HMDS) and 0.1 mL of chlorotrimethylsilane.[108] Samples were vigorously shaken for 1 min, and allowed to stand 5 min at ambient temperature. The resulting pyridinium chloride precipitate was separated by centrifugation prior to chromatographic analysis.

GC-MS work was done with a standard 25 m DB-5 (5% phenyl) column for chromatography, coupled to a time-of-flight mass spectral detector. The temperature program was 130 ˚C for 2 min, followed by a ramp to 280 ˚C at 20 ˚C/min. Routine work was done on another instrument with an FID detector.

Kinetic data were obtained using HPLC (diode array UV/Vis detection) analysis of 1 mL aliquots that were acidified with Amberlite and centrifuged before injection. A standard C18 reverse-phase column was used. The eluent was a 50:50 mixture of water and acetonitrile that contained 0.1% acetic acid. The flow was 1.0 mL/min.

Photo-Fenton reactions were set up as 100 mL solutions using 25 mL of the organic probe from a 1 mM stock solution, 10 mL of a solution containing 0.05 mM Fe^{3+} (as 0.0277 g $Fe_2(SO_4)_3$ in dilute H_2SO_4), and 1 mL (92 mM) of 30% H_2O_2. The pH was adjusted to 8.5. A rayonet lamp using 2 x 350 nm lamps was employed for photolysis. Aliquots were taken at regular time points with a crystal of sodium thiosulfate added to quench excess H_2O_2. These samples were directly injected into the HPLC for identification and quantification.

4.6 ACKNOWLEDGEMENTS

Support of this work by the National Science Foundation (CHE0518586) is gratefully acknowledged.

www.manaraa.com

4.7 REFERENCES

(1) Yu, C.; Fan, C.; Yu, J. C.; Zhou, W.; Yang, K. *Mater. Res. Bull.* **2011**, *46*, 140.

(2) Chatterjee, D.; Dasgupta, S. *Journal of Photochemistry and Photobiology C: Photochemistry Reviews* **2005**, *6*, 186.

(3) Close, K. J.; Yarwood, J. *An Introduction to Semiconductro Electronics*; 2nd ed.; Heinemann Educational Books Ltd: London, 1982.

(4) Dodd, N. J. F.; Jha, A. N.

(5) Pichat, P. *Water Science & Technology* **2007**, *55*, 167.

(6) Oh, Y.-C.; Li, X.; Cubbage, J. W.; Jenks, W. S. *Applied Catalysis B: Environmental* **2004**, *54*, 105.

(7) Suppan, P. *Principles of photochemistry*; Chemical Society: London, 1973; Vol. 22.

(8) Matthews, R. W. *Journal of Catalysis* **1988**, *111*, 264.

(9) Hong, X.; Wang, Z.; Cai, W.; Lu, F.; Zhang, J.; Yang, Y.; Ma, N.; Liu, Y. *Chem. Mater.* **2005**, *17*, 1548.

(10) Przyborski, P.; Remer, L.; Vol. 2011.

(11) Matsumoto, Y.; Katayama, M.; Abe, T.; Ohsawa, T.; Ohkubo, I.; Kumigashira, H.; Oshima, M.; Koinuma, H. *Journal of the Ceramic Society of Japan* **2010**, *118*, 993.

(12) Eslava, S.; McPartlin, M.; Thomson, R. I.; Rawson, J. M.; Wright, D. S. *Inorganic Chemistry* **2010**, *49*, 11532.

(13) Vu, A. T.; Nguyen, Q. T.; Bui, T. H. L.; Tran, M. C.; Dang, T. P.; Tran, T. K. H. *Advances in Natural Sciences: Nanoscience and Nanotechnology* **2010**, *1*, 015009/1.

(14) Su, W.; Zhang, Y.; Li, Z.; Wu, L.; Wang, X.; Li, J.; Fu, X. *Langmuir* **2008**, *24*, 3422.

(15) Rockafellow, E. M.; Stewart, L. K.; Jenks, W. S. *Applied Catalysis B: Environmental* **2009**, *91*, 554.

(16) Fujishima, A.; Zhang, X.; Tryk, D. A. *Surface Science Reports* **2008**, *63*, 515.

www.manaraa.com

(17) Grassian, V. H. *Environmental catalysis*; Taylor & Francis/CRC Press: Boca Raton, FL, 2005.

(18) Li, Y.; Wang, J.; Yao, H.; Dang, L.; Li, Z. *Journal of Molecular Catalysis A: Chemical* **2011**, *334*, 116.

(19) Zhang, X.; Zhang, L.; Xie, T.; Wang, D. *J. Phys. Chem. C* **2009**, *113*, 7371.

(20) Ai, Z.; Ho, W.; Lee, S.; Zhang, L. *Environmental Science & Technology* **2009**, *43*, 4143.

(21) Chang, X.; Huang, J.; Cheng, C.; Sui, Q.; Sha, W.; Ji, G.; Deng, S.; Yu, G. *Catalysis Communications* **2010**, *11*, 460.

(22) Chang, X.; Huang, J.; Tan, Q.; Wang, M.; Ji, G.; Deng, S.; Yu, G. *Catalysis Communications* **2009**, *10*, 1957.

(23) Gaya, U. I.; Abdullah, A. H. *Journal of Photochemistry and Photobiology C: Photochemistry Reviews* **2008**, *9*, 1.

(24) Fujishima, A.; Zhang, X.; Tryk, D. A. *Surface Science Reports* **2008**, *63*, 515.

(25) Abdullah, M.; Low, G. K.-C.; Matthews, R. W. *J. Phys. Chem.* **1990**, *94*, 6820.

(26) Long, R.; English, N. J. *J. Phys. Chem. C* **2009**, *113*, 9423.

(27) Grassian, V. H. In *Environmental Catalysis*; CRC Taylor & Francis: Boca Raton, 2005, p 307.

(28) Rockafellow, E. M.; Stewart, L. K.; Jenks, W. S. *Applied Catalysis B: Environmental* **2009**, *91*, 554.

(29) Cermenati, L.; Pichat, P.; Guillard, C.; Albini, A. *J. Phys. Chem. B* **1997**, *101*, 2650.

(30) Bernardini, C.; Cappelletti, G.; Dozzi, M. V.; Selli, E. *Journal of Photochemistry and Photobiology A: Chemistry* **2010**.

(31) Maki, Y.; Sako, M.; Oyabu, I.; Murase, T.; Kitade, Y.; Hirota, K. *J. Chem. Soc, Chem. Commun.* **1989**, 1780.

(32) Ranchella, M.; Rol, C.; Sebastiani, G. V. *J. Chem. Soc., Perkin Trans. 2* **2000**, 311.

(33) Ohno, T.; Mitsui, T.; Matsumura, M. *Chem. Lett.* **2003**, *32*, 364.

www.manaraa.com

(34) Ohno, T.; Tsubota, T.; Toyofuku, M.; Inaba, R. *Catal. Lett.* **2004**, *98*, 255.

(35) Vakros, J.; Kordulis, C.; Lycourghiotis, A. *Chem. Commun.* **2002**, 1980.

(36) Abdullah, M. L., L.; Matthews, R. W. *J. Phys. Chem.* **1990**, *94*, 6820.

(37) Song, S.; Tu, J.; Xu, L.; Xu, X.; He, Z.; Qiu, J.; Ni, J.; Chen, J. *Chemosphere* **2008**, *73*, 1401.

(38) Tojo, S.; Tachikawa, T.; Fujitsuka, M.; Majima, T. *J. Phys. Chem. C* **2008**, *112*, 14948.

(39) Liu, G.; Chen, Z.; Dong, C.; Zhao, Y.; Li, F.; Lu, G. Q.; Cheng, H.-M. *J. Phys. Chem. B* **2006**, *110*, 20823.

(40) Kuznetsov, V. N.; Serpone, N. *J. Phys. Chem. B* **2006**, *110*, 25203.

(41) Thompson, T. L.; Yates, J. T. *Topics in Catalysis* **2005**, *35*, 197.

(42) Emeline, A. V.; Sheremetyeva, N. V.; Khomchenko, N. V.; Ryabchuk, V. K.; Serpone, N. *J. Phys. Chem. C* **2007**, *111*, 11456.

(43) Devi, L. G.; Kumar, S. G. *Appl. Surf. Sci.* **2011**, *257*, 2779.

(44) Choi, J.; Park, H.; Hoffmann, M. R. *J. Mater. Res.* **2010**, *25*, 149.

(45) Sakthivel, S.; Kisch, H. *Angew. Chem., Int. Ed.* **2003**, *42*, 4908.

(46) Khan, S. U. M.; Al-Shahry, M.; Ingler, W. B., Jr. *Science (Washington, DC, U. S.)* **2002**, *297*, 2243.

(47) Lei, Y.; Wang, G.; Song, S.; Fan, W.; Pang, M.; Tang, J.; Zhang, H. *Dalton Trans.* **2010**, *39*, 3273.

(48) Chang, X.; Huang, J.; Tan, Q.; Wang, M.; Ji, G.; Deng, S.; Yu, G. *Catal. Commun.* **2009**, *10*, 1957.

(49) Hosmane, R.; Liebman, J. *Structural Chemistry* **2009**, *20*, 693.

(50) Izumi, I.; Fan, F. F.; Bard, A. J. *J. Phys. Chem.* **1981**, *85*, 218.

(51) Okamoto, K.; Yamamoto, Y.; Tanaka, H.; Tanaka, M.; Itaya, A. *Bull. Chem. Soc. Jpn.* **1985**, *58*, 2015.

(52) Fox, M. A.; Dulay, M. T. *Chem. Rev.* **1993**, *93*, 341.

(53) Fox, M. A. In *Photocatalytic Purification and Treatment of Water and Air*; Ollis, D. F., Al-Ekabi, H., Eds.; Elsevier: 1993; Vol. 3, p 163.

(54) Legrini, O.; Oliveros, E.; Braun, A. M. *Chem. Rev.* **1993**, *93*, 671.

www.manaraa.com

(55) Mallard-Dupuy, C.; Guillard, C.; Courbon, H.; Pichat, P. *Environ. Sci. Technol.* **1994**, *28*, 2176.

(56) Hoffmann, M. R.; Martin, S. T.; Choi, W.; Bahnemann, D. W. *Chem. Rev.* **1995**, *95*, 69.

(57) Qamar, M.; Muneer, M.; Bahnemann, D. *Res. Chem. Int.* **2005**, *31*, 807.

(58) Jenks, W. S. In *Environmental Catalysis*; Grassian, V. H., Ed.; CRC Press: Boca Raton, 2005, p 307.

(59) Li, X.; Cubbage, J. W.; Jenks, W. S. *J. Photochem. Photobiol. A* **2001**, *143*, 69.

(60) Linsebigler, A. L.; Lu, G.; Yates, J. T., Jr. *Chem. Rev.* **1995**, *95*, 735.

(61) Sun, Y.; Pignatello, J. J. *Environ. Sci. Technol.* **1995**, *29*, 2065.

(62) Li, X.; Cubbage, J. W.; Jenks, W. S. *J. Photochem. Photobiol., A* **2001**, *143*, 69.

(63) Li, X.; Jenks, W. S. *J. Am. Chem. Soc.* **2000**, *122*, 11864.

(64) Cermenati, L.; Pichat, P.; Guillard, C.; Albini, A. *J. Phys. Chem. B* **1997**, *101*, 2650.

(65) Cermenati, L.; Albini, A.; Pichat, P.; Guillard, C. *Res. Chem. Intermed.* **2000**, *26*, 221.

(66) Enriquez, R.; Pichat, P. *Langmuir* **2001**, *17*, 6132.

(67) Ranchella, M.; Rol, C.; Sebastiani, G. V. *J. Chem. Soc. Perkin Trans. 2* **2000**, 311.

(68) Cermenati, L.; Albini, A.; Pichat, P.; Guillard, C. *Res. Chem. Int.* **2000**, *26*, 221.

(69) Rockafellow, E. M.; Fang, X.; Trewyn, B. G.; Schmidt-Rohr, K.; Jenks, W. S. *Chem. Mater.* **2009**, *21*, 1187.

(70) Rockafellow, E. M.; Haywood, J. M.; Witte, T.; Houk, R. S.; Jenks, W. S. *Langmuir* **2010**, *in press.*

(71) Rockafellow, E. M.; Stewart, L. K.; Jenks, W. S. *Appl. Catal. B* **2009**, *91*, 554.

(72) Hathway, T.; Jenks, W. S. *Journal of Photochemistry and Photobiology A: Chemistry* **2008**, *200*, 216.

www.manaraa.com

(73) Hathway, T.; Rockafellow, E. M.; Oh, Y.-C.; Jenks, W. S. *J. Photochem. Photobiol., A* **2009**, *207*, 197.

(74) Oh, Y.-C.; Li, X.; Cubbage, J. W.; Jenks William, S. *Appl. Catal. B: Environmental* **2004**, *54*, 105.

(75) Cunningham, J.; Al-Sayyed, G.; Srijaranal, S. In *Aquat. Surf. Photochem.*; Helz, G. R., Ed.; Lewis, Boca Raton, Fla: 1994, p 317.

(76) Cunningham, J.; Sedlak, P. *J. Photochem. Photobiol. A* **1994**, *77*, 255.

(77) Tunesi, S.; Anderson, M. *J. Phys. Chem.* **1991**, *95*, 3399.

(78) Li, X.; Cubbage, J. W.; Jenks, W. S. *J. Org. Chem.* **1999**, *64*, 8525.

(79) Li, X.; Cubbage, J. W.; Tetzlaff, T. A.; Jenks, W. S. *J. Org. Chem.* **1999**, *64*, 8509.

(80) Fox, M. A.; Ogawa, H.; Pichat, P. *J. Org. Chem.* **1989**, *54*, 3847.

(81) Pichat, P.; D'Oliveira, J.-C.; Maffre, J.-F.; Mas, D. In *Photocatalytic Purification and Treatment of Water and Air*; Ollis, D. F., Al-Ekabi, H., Eds.; Elsevier: 1993; Vol. 3, p 683.

(82) Enriquez, R.; Agrios, A. G.; Pichat, P. *Catal. Today* **2007**, *120*, 196.

(83) Palmisano, G.; Addamo, M.; Augugliaro, V.; Caronna, T.; Di, P. A.; Lopez, E. G.; Loddo, V.; Marci, G.; Palmisano, L.; Schiavello, M. *Catal. Today* **2007**, *122*, 118.

(84) Poerschmann, J.; Trommler, U. *J. Chromatogr., A* **2009**, *1216*, 5570.

(85) Parra, S.; Olivero, J.; Pacheco, L.; Pulgarin, C. *Appl. Catal. B* **2003**, *43*, 293.

(86) Yoshida, H.; Yuzawa, H.; Aoki, M.; Otake, K.; Itoh, H.; Hattori, T. *Chemical Communications* **2008**, 4634.

(87) Palmisano, G.; Addamo, M.; Augugliaro, V.; Caronna, T.; Di Paola, A.; LÛpez, E. G.; Loddo, V.; MarcÏ, G.; Palmisano, L.; Schiavello, M. *Catal. Today* **2007**, *122*, 118.

(88) Jefcoate, C. R. E.; Smith, J. R. L.; Norman, R. O. C. *Journal of the Chemical Society B: Physical Organic* **1969**, 1013.

(89) Jefcoate, C. R. E.; Smith, J. R. L.; Norman, R. O. C. *J. Chem. Soc. B* **1969**, 1013.

(90) Izumi, I.; Fan, F.-R. F.; Bard, A. J. *J. Phys. Chem.* **1981**, *85*, 218.

www.manaraa.com

(91) Mills, A.; Holland, C. E.; Davies, R. H.; Worsley, D. *Journal of Photochemistry and Photobiology A: Chemistry* **1994**, *83*, 257.

(92) Velegraki, T.; Mantzavinos, D. *Chemical Engineering Journal* **2008**, *140*, 15.

(93) Chan, A. H. C.; Chan, C. K.; Barford, J. P.; Porter, J. F. *Water Research* **2003**, *37*, 1125.

(94) Deng, Y.; Zhang, K.; Chen, H.; Wu, T.; Krzyaniak, M.; Wellons, A.; Bolla, D.; Douglas, K.; Zuo, Y. *Atmospheric Environment* **2006**, *40*, 3665.

(95) Matthews, R. W. *Water Res.* **1986**, *20*, 569.

(96) De Laat, J.; Gallard, H. *Environ. Sci. Technol* **1999**, *33*, 2726.

(97) Pignatello, J. *Environ. Sci. Technol.* **1992**, *26*, 944.

(98) Ensing, B.; Buda, F.; Blöchl, P.; Baerends, E. J. *Angew. Chem. Int. Ed.* **2001**, *40*, 2893.

(99) Zepp, R. G.; Faust, B. C.; Hoigné, J. *Environ. Sci. Technol.* **1992**, *26*, 313.

(100) Ilisz, I. n.; Dombi, A. s. *Appl. Catal. A* **1999**, *180*, 35.

(101) Minero, C.; Mariella, G.; Maurino, V.; Pelizzetti, E. *Langmuir* **2000**, *16*, 2632.

(102) Minero, C.; Mariella, G.; Maurino, V.; Vione, D.; Pelizzetti, E. *Langmuir* **2000**, *16*, 8964.

(103) Benoit-Marquié, F.; Puech-Costes, E.; Braun, A. M.; Oliveros, E.; Maurette, M.-T. *J. Photochem. Photobiol. A* **1997**, *108*, 65.

(104) Waldo, J. P.; Larock, R. C. *Org. Lett.* **2005**, *7*, 5203.

(105) Fujishiro, K.; Mitamura, S. *Bull. Chem. Soc. Japan* **1988**, *61*, 4464.

(106) Hatchard, C. G.; Parker, C. A. *Proc. Royal. Soc. A* **1956**, *235*, 518.

(107) Bowman, W. D.; Demas, J. N. *J. Phys. Chem.* **1976**, *80*, 2434.

(108) Sweeley, C. C.; Bentley, R.; Makita, M.; Wells, W. W. *J. Am. Chem. Soc.* **1963**, *85*, 2497.

4.8 SUPPORTING INFORMATION

The supporting information for this paper may be found in the Appendix.

www.manaraa.com

Chapter 5: Conclusions

In this thesis potential visible light photocatalysts have been explored. Though neither the iodine modified titanium dioxide nor the bismuth oxyiodide are efficient or robust enough to solve the growing global pollution problem, studying them has lead to some important advancements. Though it was shown that though both catalysts are exceptionally efficient at degrading phenol, they lack the ability to degrade a wide variety of pollutants, which is necessary for a superior pollutant remediation catalyst, there have been great successes.

Iodine modified titanium dioxide has been shown to be tunable through the annealing process, with different annealing temperatures leading to a change in degradation pathway used by the catalyst. This could potentially allow these catalysts to be altered so that toxic intermediates produced by one degradation pathway could be avoided or minimized. This fact can also be used to make the catalysts more capable of degrading specific pollutants. Since SET chemistry requires adsorption onto the catalyst's surface, poorly binding substrates may be more readily degraded by the catalysts that proffer hydroxyl chemistry.

While studying iodine modified titanium dioxide, evidence to support the theory that defects in the crystal lattice are responsible for the catalytic behavior rather than the dopants was gathered as a sample containing no iodine behaved similarly to the samples that did contain iodine. This suggests that it may be possible to reduce the amount of dopant used in producing the catalysts without reducing their catalytic ability. Besides the obvious cost reduction benefit, this may also decrease the hazards associated with dopant leaching and permit the use of more expensive dopants that could enhance catalytic ability but would generally be too expensive to investigate if high concentrations were used.

In both the case of iodine modified titanium dioxide and bismuth oxyiodide, the oxidative potential of the catalysts must be determined. They both show exceptional efficiency with phenol but lack efficiency with other probe molecules. The next logical step is to determine what pollutants they can degrade efficiently so that we know their strengths and weaknesses so that we can make educated attempts to improve them. To do this, more probes are needed, and though the potential probe molecules discussed in Chapter 4 may not

www.manaraa.com

have been perfect, studies into others is necessary for once we determine what the oxidative ability of these catalysts are, we will be able to make an honest assessment of their utility. For now, we know that they have great potential, but cannot determine how great.

www.manaraa.com

Appendix

Materials. Compounds **1**, **1c**, 4-iodobenzoic acid, 5-iodosalicylic acid, and phenylboronic acid were used as obtained from Sigma-Aldrich. 4-Iodosalicylic acid was used as obtained from Trans World Chemicals. The 2-, 3-, and 4-formylphenylboronic acids were used as obtained from Frontier Scientific. NMR spectra were obtained on a 300 or 400 MHz instrument, and HRMS data were obtained with a solids probe using CI with methane as the ionizing gas.

Chart S1. Compounds synthesized and/or used in this study.

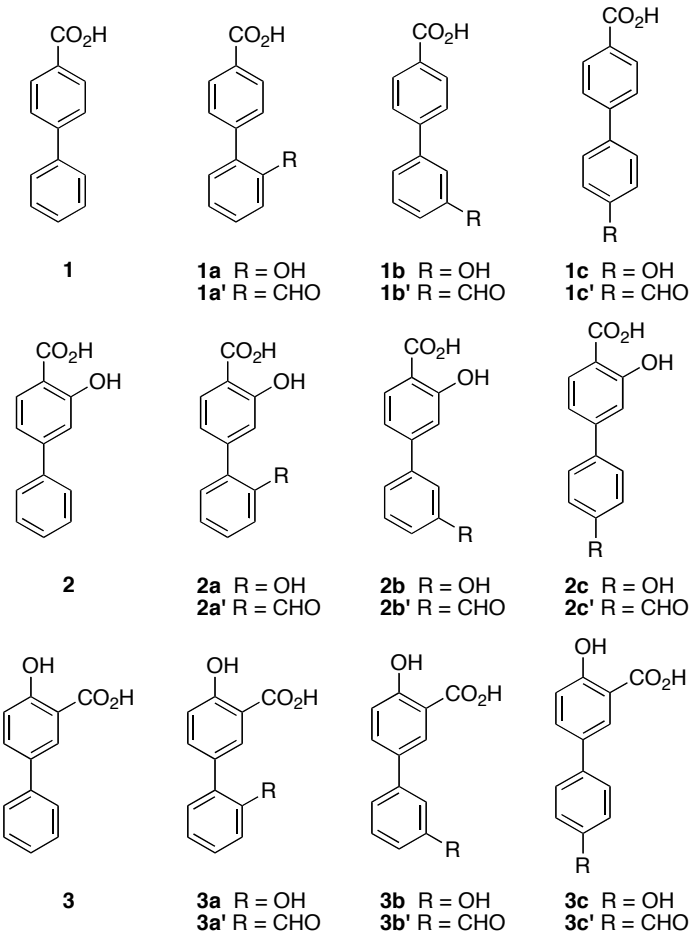

Preparation of 2 and 3. Scheme 1 shows the general Suzuki-Miyaura coupling scheme used to form the compounds in Chart 1, with **3** used as an example. To a vial, 1 equiv. (2 mmol) of aryl iodide, 1.3 equiv. of aryl boronic acid, 3.4 equiv. of $KHCO_3$ and 0.02 equiv. of

www.manaraa.com

$PdCl_2$ were added and dissolved in 10 mL of 4:1 DMF/H_2O. After purging with Ar for 5 min, the mixture was heated and stirred at 85˚C for 24 h (or longer based on TLC). Completed reactions were acidified with 10% HCl, washed with thiosulfate to remove iodides, and then extracted into EtOAc. The organic layer was then washed with water three times to remove DMF, followed by a final washing with saturated aqueous NaCl. The organic layer was then dried over Na_2SO_4 before removal of the solvent *in vacuo*. Crude ^{1}H-NMR spectroscopy was used to look for a clean product. If little or no starting materials were present, the product was recrystallized from EtOH/H_2O. If aryl boronic acids persisted, column chromatography with 1:1 hexanes:EtOAc was used to remove them. The products were then eluted with 10% MeOH in EtOAc, followed by MeOH.

Scheme S1. Suzuki-Miyaura coupling to prepare **3**.

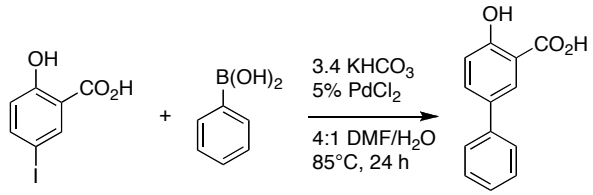

3

4-Phenylsalicylic acid (2): 238 mg (43%), unoptimized; ^{1}H-NMR (CD_3OD, 400 MHz) δ 7.14 (d, *J* = 8.4 Hz, 1H), 7.16 (s, 1H), 7.37 (t, *J* = 7.2 Hz, 1H), 7.44 (t, *J* = 7.2 Hz, 2H), 7.62 (d, *J* = 7.2 Hz, 2H) 7.90 (d, *J* = 8.4 Hz, 1 H); ^{13}C-NMR (CD_3OD, 400 MHz) δ 112.8, 116.3, 119.0, 128.3, 129.6, 130.1, 132.2, 141.2, 149.8, 163.6, 173.6. HRMS (M+1) 215.0708 calcd, 215.0699 observed.

5-Phenylsalicylic acid (3): 479 mg (86%), unoptimized; ^{1}H-NMR (CD_3OD, 400 MHz) δ 7.01 (d, *J* = 8.8 Hz, 1H), 7.29 (t, *J* = 7.6 Hz, 1H), 7.40 (t, *J* = 7.2 Hz, 2H), 7.53 (d, *J* = 7.6 Hz, 2H), 7.72 (dd, *J* = 8.4, 2.4 Hz, 1H) 8.08 (d, *J* = 2.4 Hz, 1 H); ^{13}C-NMR (CD_3OD, 400 MHz) δ 114.2, 118.9, 127.6, 128.2, 129.7, 130.1, 133.7, 135.3, 141.4, 162.8, 173.6. HRMS (M+1) 215.0708 calcd, 215.0704 observed.

Preparation of hydroxylated biphenyls (1a, 1b, 2a-c, and 3a-3c). Each hydroxylated biphenyl was prepared in two steps using the appropriate formylboronic acid using the above

www.manaraa.com

procedure, followed by a Baeyer-Villiger oxidation of the resulting biphenyl aldehyde. The preparation of **3a** is shown as an example in Scheme 2.[105] For the oxidation, 1 equiv. (100 mg) of aldehyde, 1.2 equiv. of MCPBA and dry CH_2Cl_2 (5 mL for each mmol aldehyde) were added to a flame-dried flask and then stirred under Ar overnight. If the oxidation was not complete by TLC, it was heated to reflux for 30 min. MeOH (10 mL) and 10% KOH (10 mL) were then added and stirred for 1 h to hydrolyze the ester, and then the methanol was removed by rotary evaporation. The mixture was then acidified and extracted with ethyl acetate, followed by washes with water and saturated aqueous NaCl. The solvent was completely removed by rotary evaporation. Column chromatography was employed using 19:1 hexanes:EtOAc to remove *meta*-chlorobenzoic acid, followed by 10% MeOH in EtOAc and MeOH to elute the product, which was then recrystallized from MeOH/H_2O. The raw ^{1}H-NMR, and ^{13}C-NMR spectra are given below. Two step percent yields are given, and each preparation was unoptimized. Additionally, since these compounds were meant as authentic samples for chromatographic and mass spectral confirmation of structures, rather than as clean starting materials, the raw NMR data show small amounts of impurities that were of no concern for our purposes in some instances. Tabular ^{1}H-NMR spectral data for the aldehyde intermediates (1a', etc.) are given at the end of each entry for the corresponding acids.

Scheme S2. Preparation of hydroxylated compounds (**3a** shown)

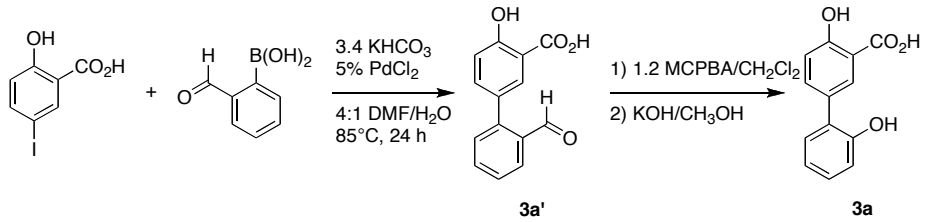

2'-Hydroxybiphenyl-4-carboxylic acid (1a): 56 mg (8%); ^{1}H-NMR (CD_3OD, 400 MHz) δ 7.39 (d, *J* = 7.2 Hz, 1H), 7.42 (d, *J* = 8.4 Hz, 2H), 7.48 (t, *J* = 7.2 Hz, 1H), 7.59 (t, *J* = 7.6 Hz, 1H), 7.87 (d, *J* = 8.0 Hz, 1H), 8.04 (d, *J* = 8.4 Hz, 2H); ^{13}C-NMR (CD_3OD, 400 MHz) δ 129.0, 129.9, 130.6, 130.7, 131.1, 131.9, 132.6, 132.9, 143.0, 147.9, 169.9, 171.8; HRMS (M+1) 215.0708 calcd, 215.0720 observed. **1a'** ^{1}H-NMR (CD_3OD, 300 MHz) δ 7.48 (d, *J* =

www.manaraa.com

7.0 Hz, 1H), 7.50 (d, *J* = 8.4 Hz, 2H), 7.56 (t, *J* = 7.5 Hz, 1H), 7.59 (td, *J* = 7.5, 1.2 Hz, 1H), 7.98 (dd, *J* = 7.8, 1.2 Hz, 1H), 8.11 (d, *J* = 8.4 Hz, 2H), 9.90 (s, 1H).

3'-Hydroxybiphenyl-4-carboxylic acid (1b): 28 mg (2%); ^{1}H-NMR (CD_3OD, 300 MHz) δ 7.59 (t, *J* = 7.2 Hz, 1H), 7.77 (d, *J* = 8.4 Hz, 2H), 7.92 (d, *J* = 7.5 Hz, 1H), 8.05 (d, *J* = 7.5 Hz, 1H), 8.14 (d, *J* = 8.7 Hz, 2H) 8.32 (s, 1H); ^{13}C-NMR (CD_3OD, 400 MHz) δ 126.7, 127.9, 128.9, 129.0, 130.1, 131.2, 131.8, 140.2, 144.4, 168.4; HRMS (M+1) 215.0708 calcd, 215.0710 observed. **1b'** ^{1}H-NMR (CD_3OD, 300 MHz) δ 7.68 (t, *J* = 7.2 Hz, 1H), 7.80 (d, *J* = 8.4 Hz, 2H), 7.94 (d, *J* = 7.5 Hz, 1H), 7.99 (d, *J* = 7.5 Hz, 1H), 8.12 (d, *J* = 8.7 Hz, 2H) 8.20 (s, 1H), 10.07 (s, 1H).

2',3-Dihydroxybiphenyl-4-carboxylic acid (2a): 352 mg (51%); ^{1}H-NMR (CD_3OD, 400 MHz) δ 6.90 (t, *J* = 7.2 Hz, 2H), 7.11 (d, *J* = 8.4 Hz, 1H), 7.14 (s, 1H), 7.18 (t, *J* = 7.6 Hz, 1H), 7.27 (d, *J* = 7.6 Hz, 1H) 7.85 (d, *J* = 8.4 Hz, 1H); ^{13}C-NMR (CD_3OD, 400 MHz) δ 112.1, 117.2, 118.8, 121.1, 121.6, 128.5, 130.5, 131.1, 131.5, 148.1, 155.6, 162.8, 173.6; HRMS (M+1) 231.0657 calcd, 231.0656. observed. **2a'** ^{1}H-NMR (CD_3OD, 300 MHz) δ 6.87 (t, *J* = 7.2 Hz, 2H), 7.24 (m, 1H), 7.37 (m, 2H), 7.62 (d, *J* = 7.6 Hz, 1H) 7.89 (d, *J* = 8.4 Hz, 1H), 9.94 (s, 1H).

3,3'-Dihydroxybiphenyl-4-carboxylic acid (2b): 15 mg (1%); ^{1}H-NMR (CD_3OD, 400 MHz) δ 7.17 (s, 2H), 7.58 (t, *J* = 8.4 Hz, 1H), 7.88 (d, *J* = 8.0 Hz, 1H), 7.95 (d, *J* = 7.6 Hz, 1H), 8.04 (d, *J* = 7.2 Hz, 1H), 8.28 (s, 1H); HRMS (M+1) HRMS (M+1) 231.0657 calcd, 231.0660 observed. ^{13}C-NMR (CD_3OD, 400 MHz) δ 116.3, 118.9, 129.4, 130.4, 130.6, 132.5, 132.8, 132.9, 141.7, 142.0, 148.1, 163.6, 169.8; **2b'** ^{1}H-NMR (CD_3OD, 300 MHz) δ 7.17 (s, 2H), 7.68 (t, *J* = 7.8 Hz, 1H), 7.96 (m, 3H), 8.19 (s, 1H), 10.07 (s, 1H).

3,4'-Dihydroxybiphenyl-4-carboxylic acid (2c): 62 mg (18%); ^{1}H-NMR (CD_3OD, 400 MHz) δ 6.86 (d, *J* = 8.4 Hz, 2H), 7.07 (d, *J* = 8.4 Hz, 1H), 7.09 (s, 1H), 7.48 (d, *J* = 8.8 Hz, 2H), 7.84 (d, *J* = 8.8 Hz, 1 H); ^{13}C-NMR (CD_3OD, 400 MHz) δ 111.9, 115.3, 116.9, 118.4, 129.4, 132.0, 132.2, 149.7, 159.3. 163.5, 173.6; HRMS (M+1) 231.0657 calcd, 231.0652 observed. **2c'** ^{1}H-NMR (CD_3OD, 300 MHz) δ 7.20 (m, 2H), 7.85 (d, *J* = 8.4 Hz, 2H), 7.93 (m, 1H) 7.98 (d, *J* = 8.4 Hz, 2H), 10.02 (s, 1H).

www.manaraa.com

2',4-Dihydroxybiphenyl-3-carboxylic acid (3a): 217 mg (31%); ^{1}H-NMR (CD_3OD, 400 MHz) δ 6.83 (d, *J* = 8.1 Hz, 1H), 6.85 (t, *J* = 6.6 Hz, 1H), 6.91 (d, *J* = 8.7 Hz, 1H), 7.09 (t, *J* = 7.5 Hz, 1H), 7.18 (d, *J* = 8.1 Hz, 2H), 7.66 (d, *J* = 8.7 Hz, 1H), 8.01 (s, 1H); ^{13}C-NMR (CD_3OD, 400 MHz) δ 113.5, 117.0, 117.8, 121.1, 128.8, 129.5, 131.4, 131.4, 132.2, 138.0, 155.5, 162.1, 173.8; HRMS (M+1) 231.0657 calcd, 231.0654 observed. **3a'** ^{1}H-NMR (CD_3OD, 300 MHz) δ 7.03 (d, *J* = 8.4 Hz, 1H), 7.49 (m, 2H), 7.67 (t, *J* = 7.5 Hz, 2H), 7.82 (d, *J* = 2.4 Hz, 1H), 7.93 (d, 8.4 Hz, 1H), 9.91 (s, 1H).

3',4-Dihydroxybiphenyl-3-carboxylic acid (3b): 44 mg (4%); ^{1}H-NMR (CD_3OD, 400 MHz) δ 7.02 (d, *J* = 8.4 Hz, 1H), 7.53 (t, *J* = 8.0, 1H), 7.56 (dd, *J* = 8.4, 2.4 Hz, 1H), 7.82 (d, *J* = 7.6 Hz, 1H), 7.96 (d, *J* = 7.6 Hz, 1H), 8.15 (d, *J* = 2.4 Hz, 1 H), 8.23 (s, 1H); ^{13}C-NMR (CD_3OD, 400 MHz) δ 112.9, 113.5, 117.3, 127.2, 127.7, 128.4, 128.8, 130.6, 130.7, 133.0, 140.5, 161.6, 168.5; HRMS (M+1) 231.0657 calcd, 231.0648 observed. **3b'** ^{1}H-NMR (CD_3OD, 400 MHz) δ 7.16 (d, *J* = 8.4 Hz, 1H), 7.67 (t, *J* = 8.0 1H), 7.95 (m, 3H), 8.00 (s, 1H), 8.19 (s, 1H), 10.05 (s, 1H).

4,4'-Dihydroxybiphenyl-3-carboxylic acid (3c): 101 mg (25%); ^{1}H-NMR (CD_3OD, 400 MHz) δ 6.84 (d, *J* = 8.8 Hz, 2H), 6.96 (d, *J* = 8.8 Hz, 1H), 7.39 (t, *J* = 8.8 Hz, 2H), 7.66 (dd, *J* = 2.4, 8.4 Hz, 1H), 8.01 (d, *J* = 2.4 Hz, 1H); ^{13}C-NMR (CD_3OD, 400 MHz) δ 114.7, 116.8, 118.6, 128.7, 129.0, 133.0, 133.7, 134.6, 158.1, 162.1, 173.9; HRMS (M+1) 231.0657 calcd, 231.0648 observed. **3c'** ^{1}H-NMR (CD_3OD, 300 MHz) δ 7.00 (d, *J* = 8.7 Hz, 1H), 7.46 (d, *J* = 6.9 Hz, 2H), 7.57 (d, *J* = 6.6 Hz, 2H), 7.75 (dd, *J* = 2.4, 8.7 Hz, 1H), 8.09 (d, *J* = 2.4 Hz, 1H), 9.99, (s, 1H).

www.manaraa.com

Compound **1a**

^{1}H-NMR (CD_3OD); Identified impurities: acetone, ethyl acetate, hexanes, water

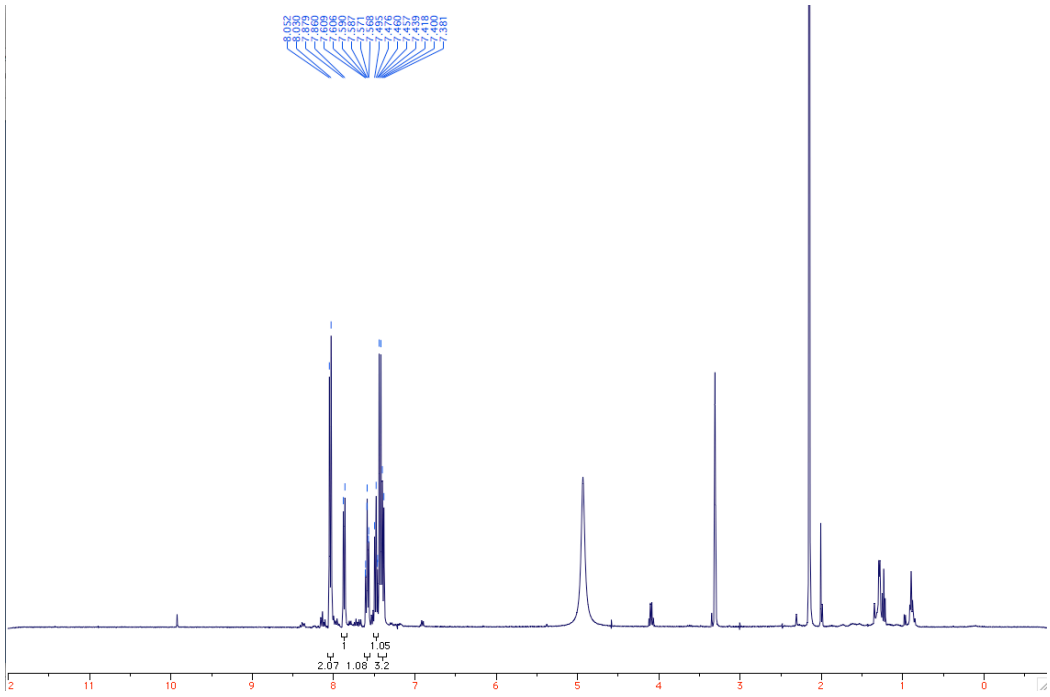

www.manaraa.com

^{13}C-NMR (CD_3OD); Identified impurities: acetone, hexanes

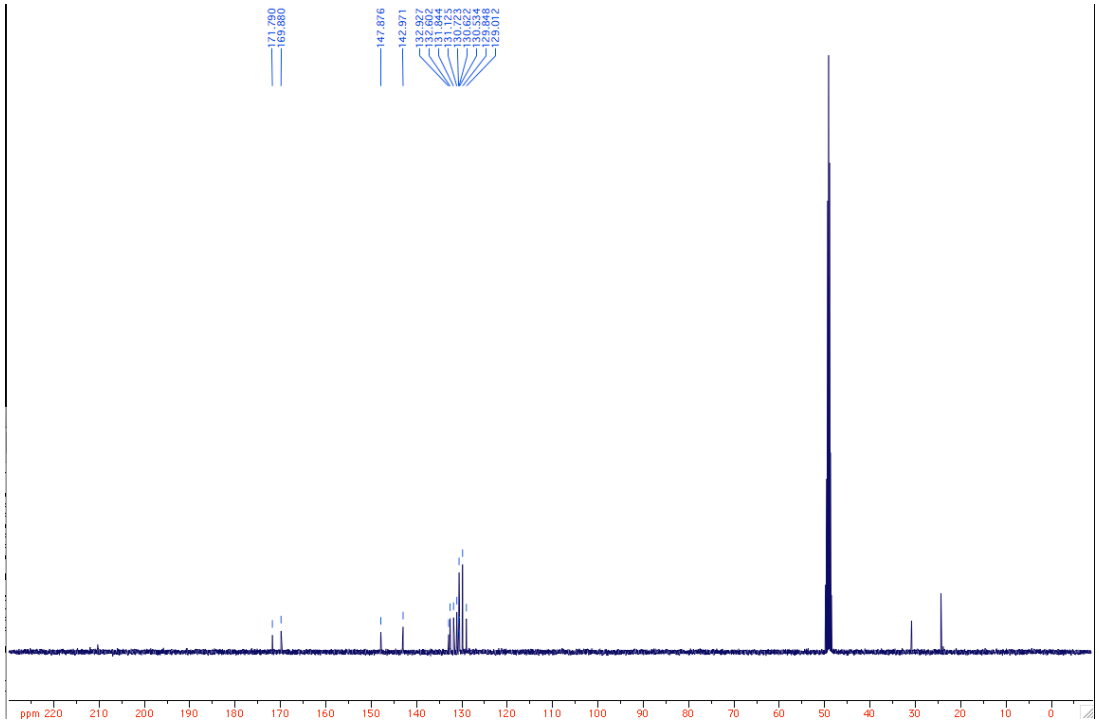

www.manaraa.com

Compound **1b**

^{1}H-NMR (CD_3OD)

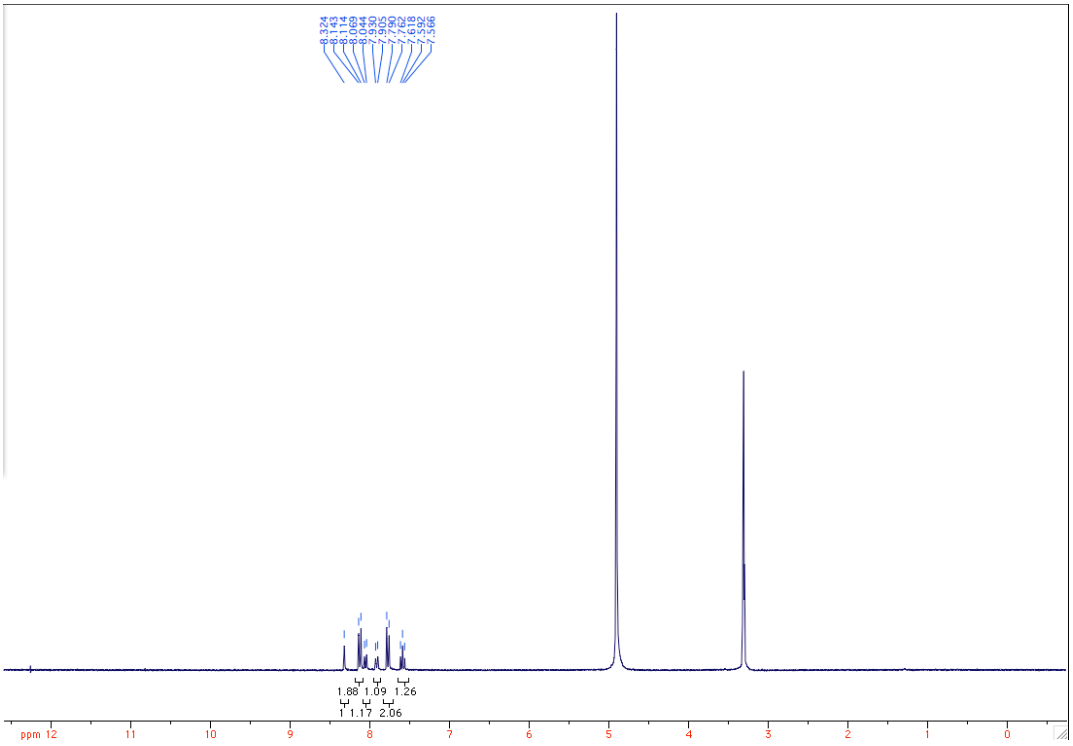

www.manaraa.com

^{13}C-NMR (CD_3OD)

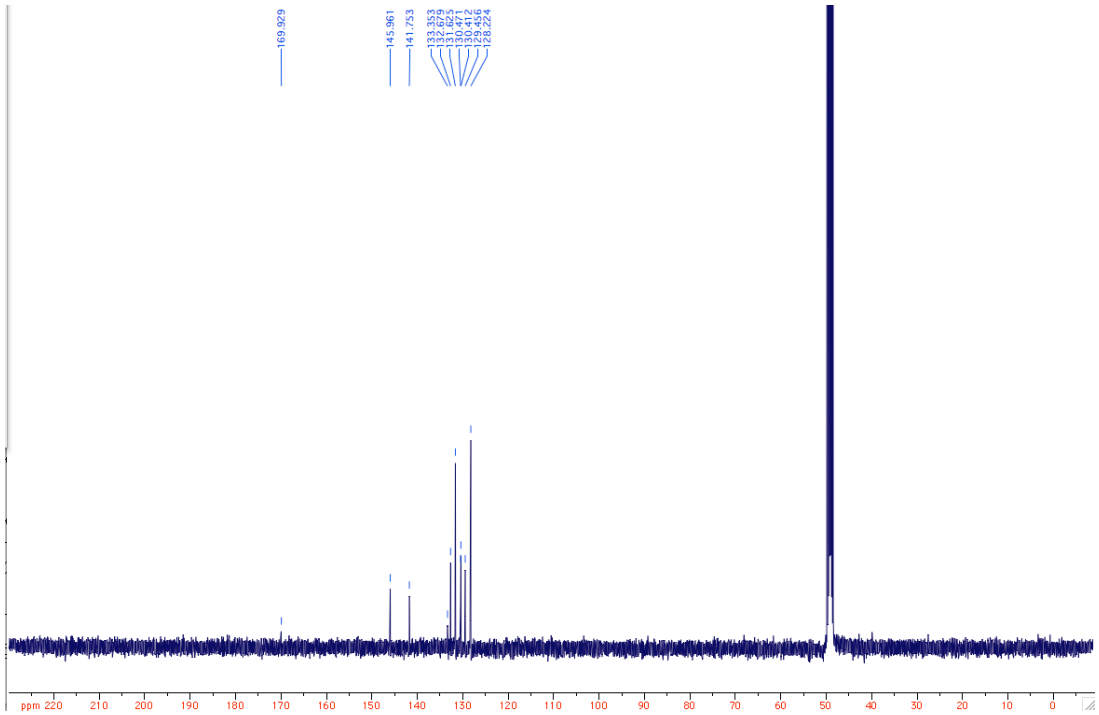

www.manaraa.com

Compound **2**

^{1}H-NMR (CD_3OD)

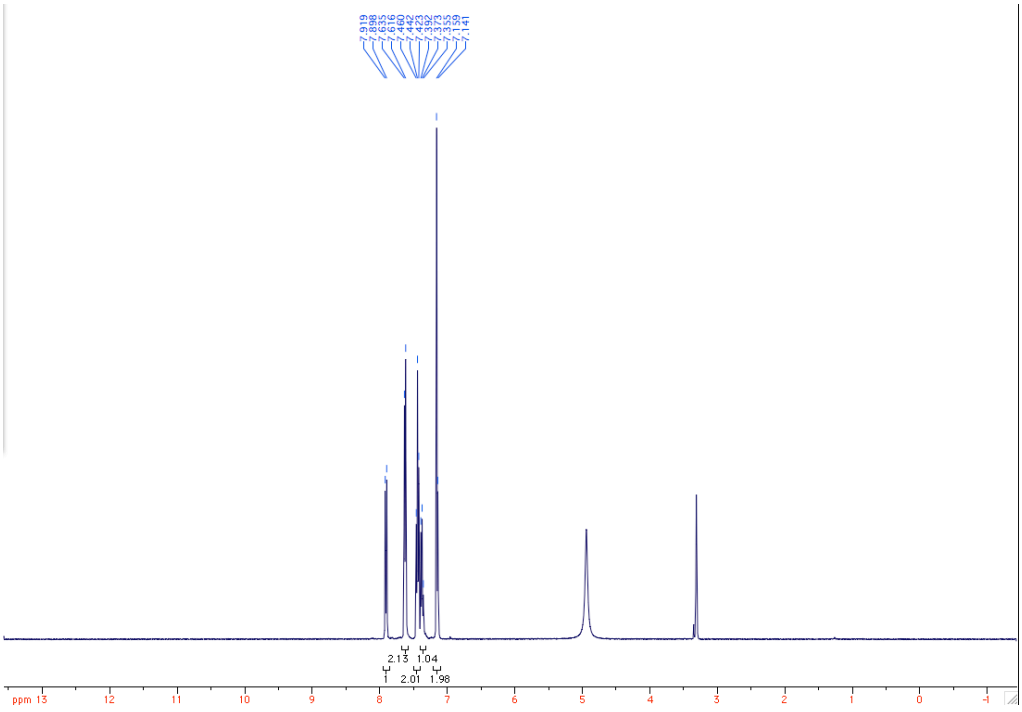

www.manaraa.com

^{13}C-NMR (CD_3OD)

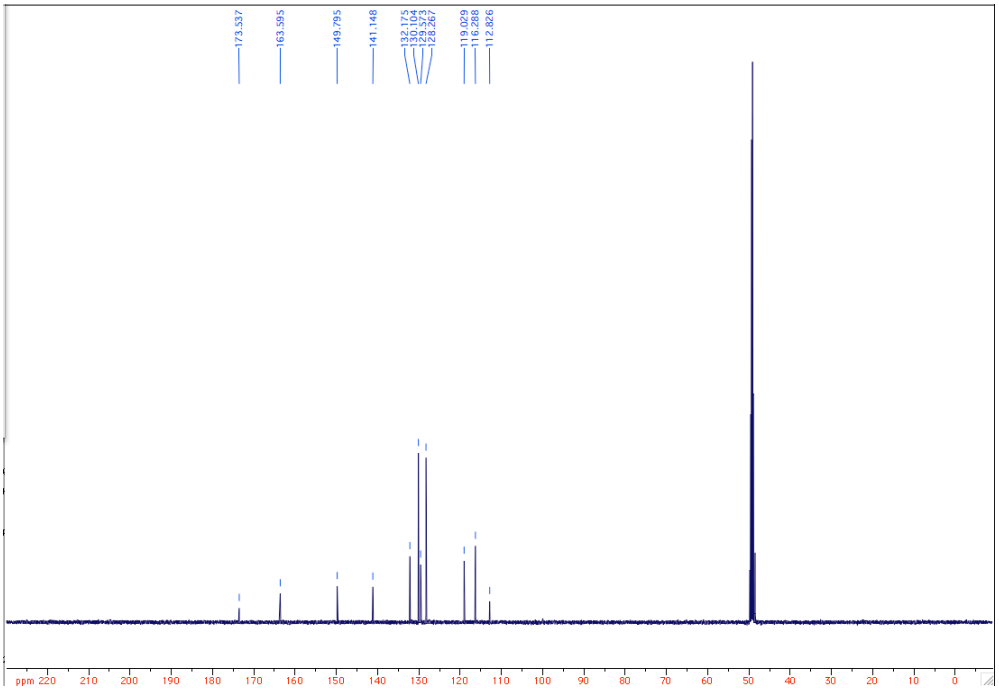

www.manaraa.com

Compound **2a**

^{1}H-NMR (CD_3OD); Identified impurities: ethanol

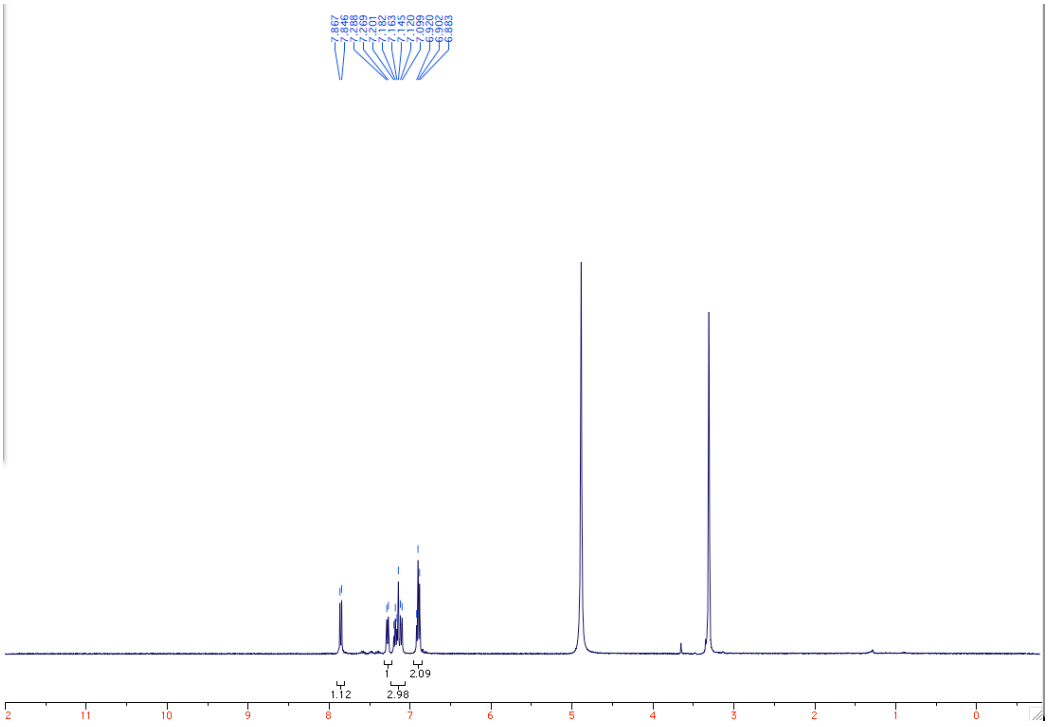

www.manaraa.com

^{13}C-NMR (CD_3OD)

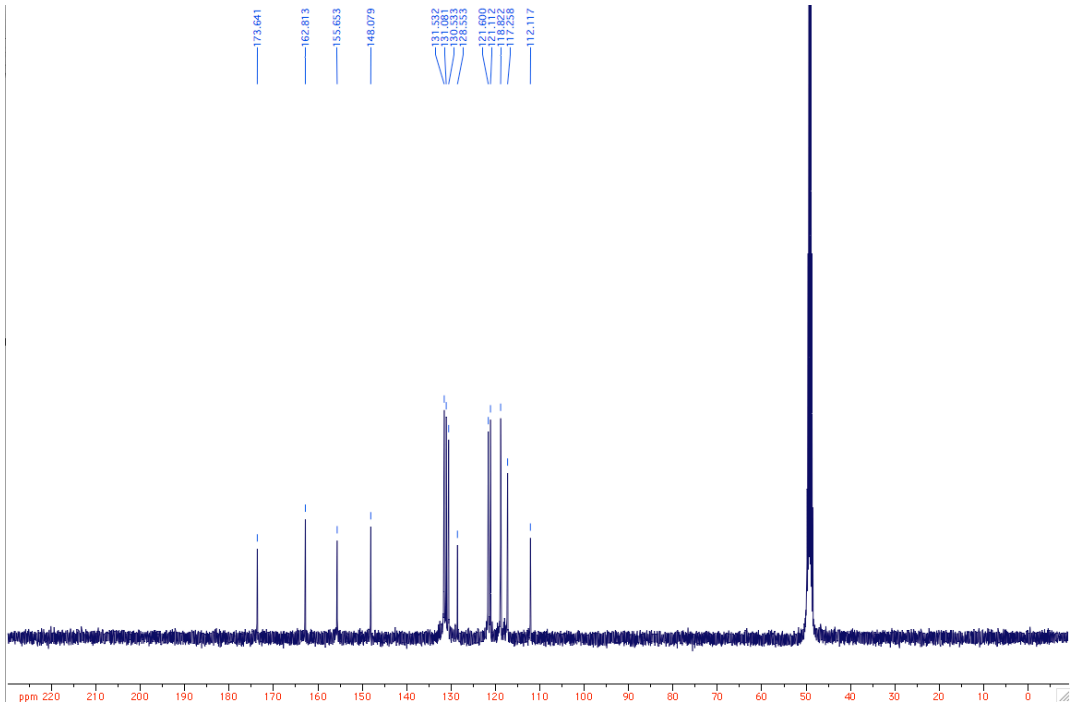

www.manaraa.com

Compound **2b**

^{1}H-NMR (CD_3OD); Identified impurities: hexane

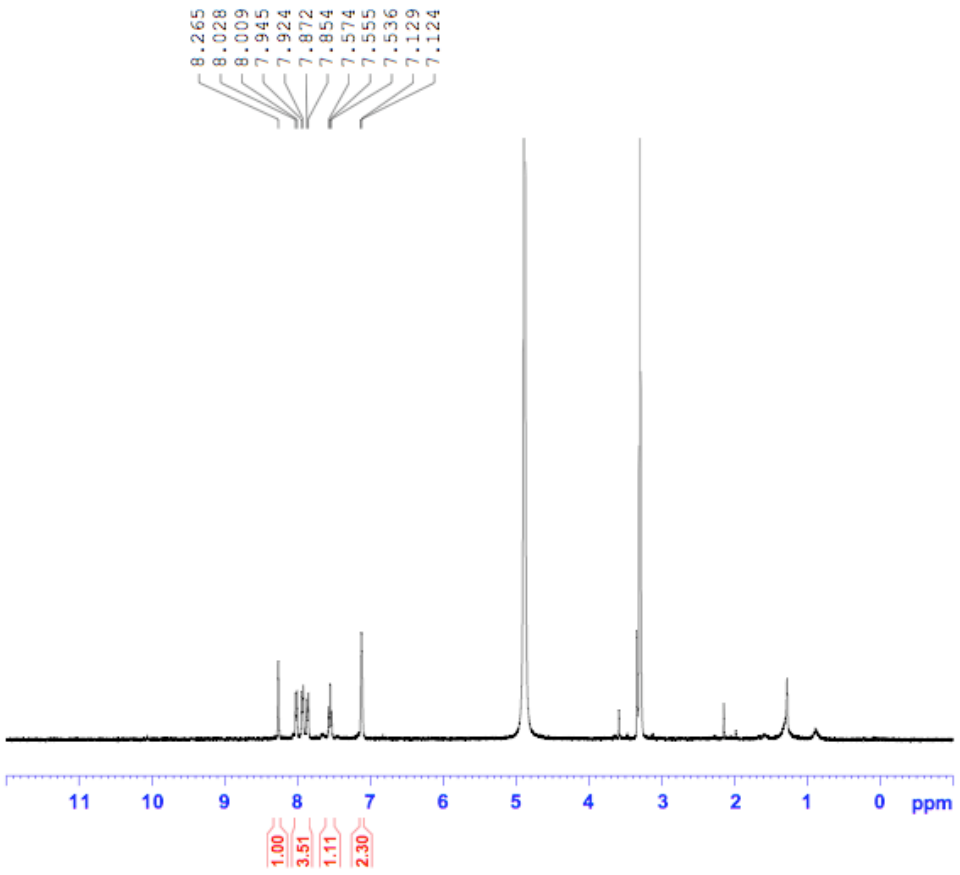

www.manaraa.com

^{13}C-NMR (CD_3OD)

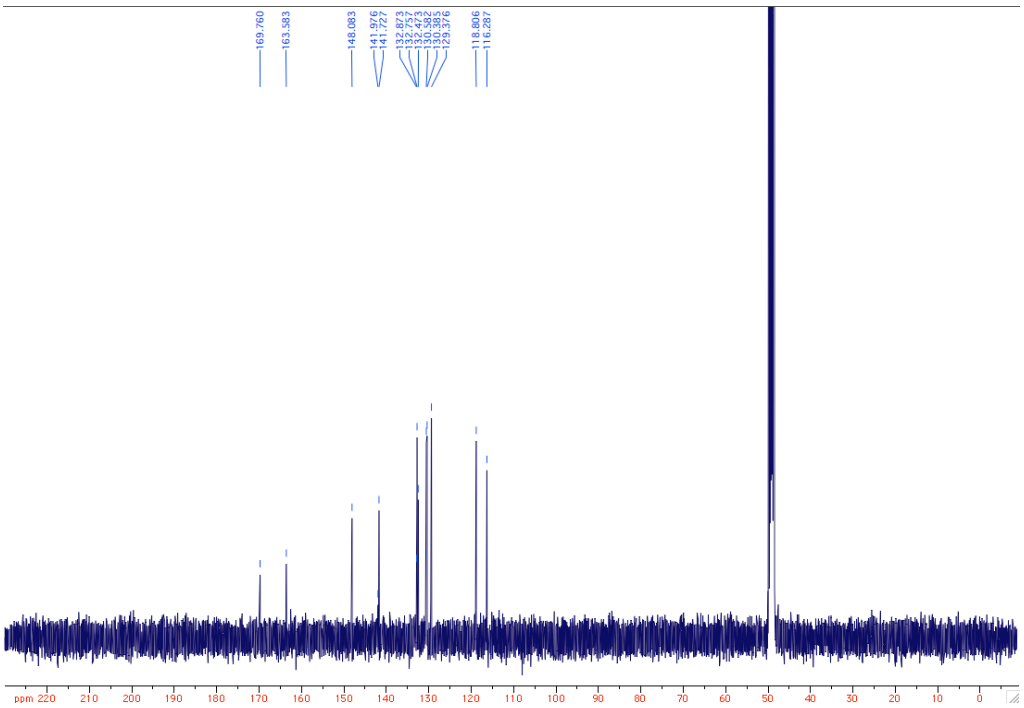

www.manaraa.com

Compound **2c**

^{1}H-NMR (CD_3OD); Identified impurities: hexanes, water

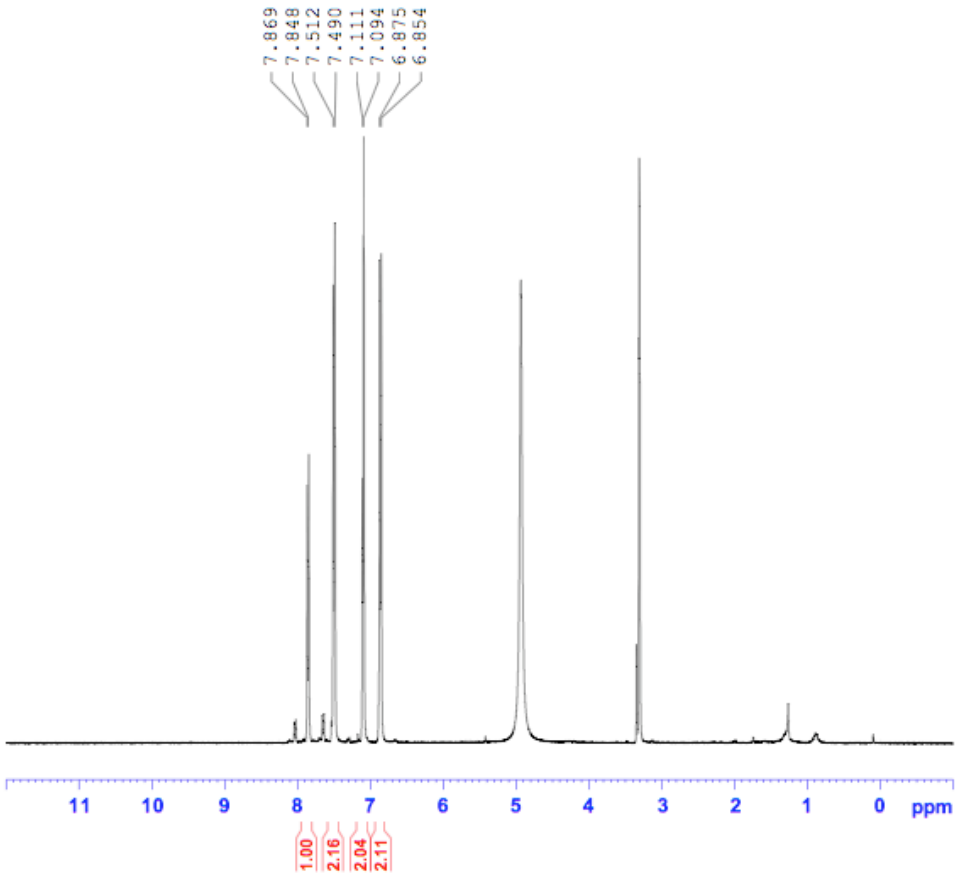

www.manaraa.com

^{13}C-NMR (CD_3OD); Identified impurities: acetone, ethyl acetate, hexanes

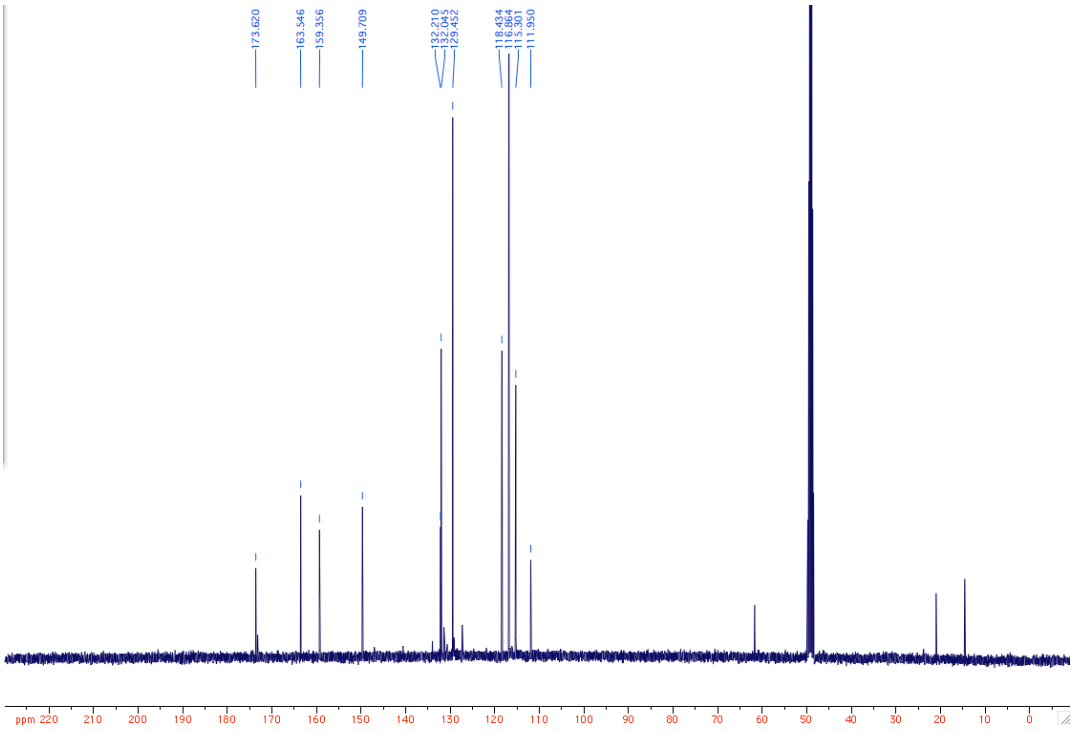

www.manaraa.com

Compound **3**

^{1}H-NMR (CD_3OD); Identified impurities: ethanol

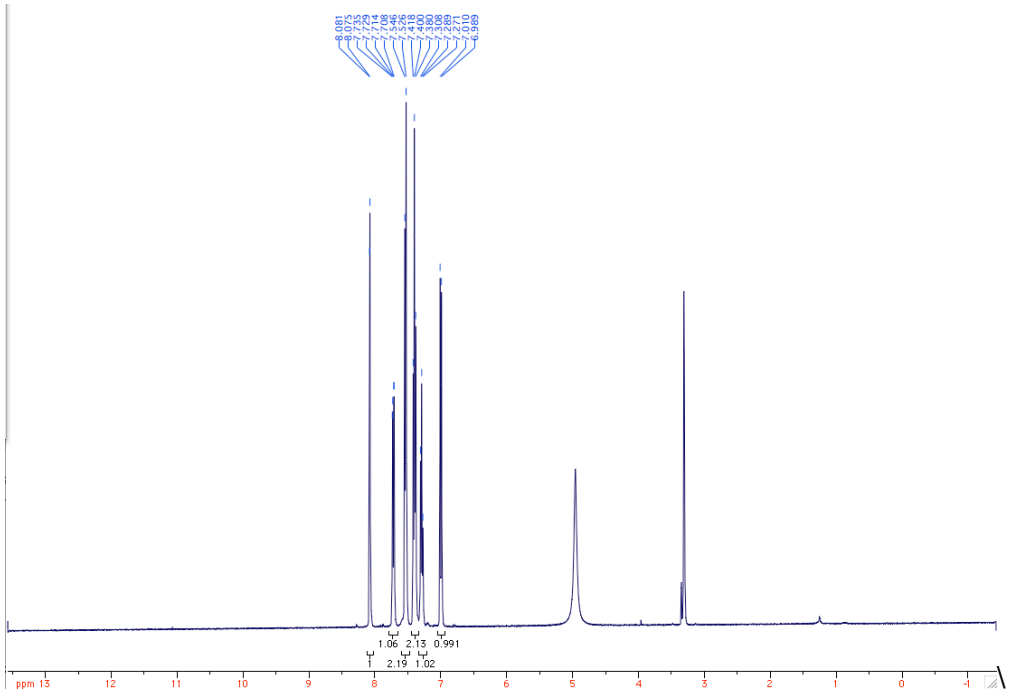

www.manaraa.com

^{13}C-NMR (CD_3OD)

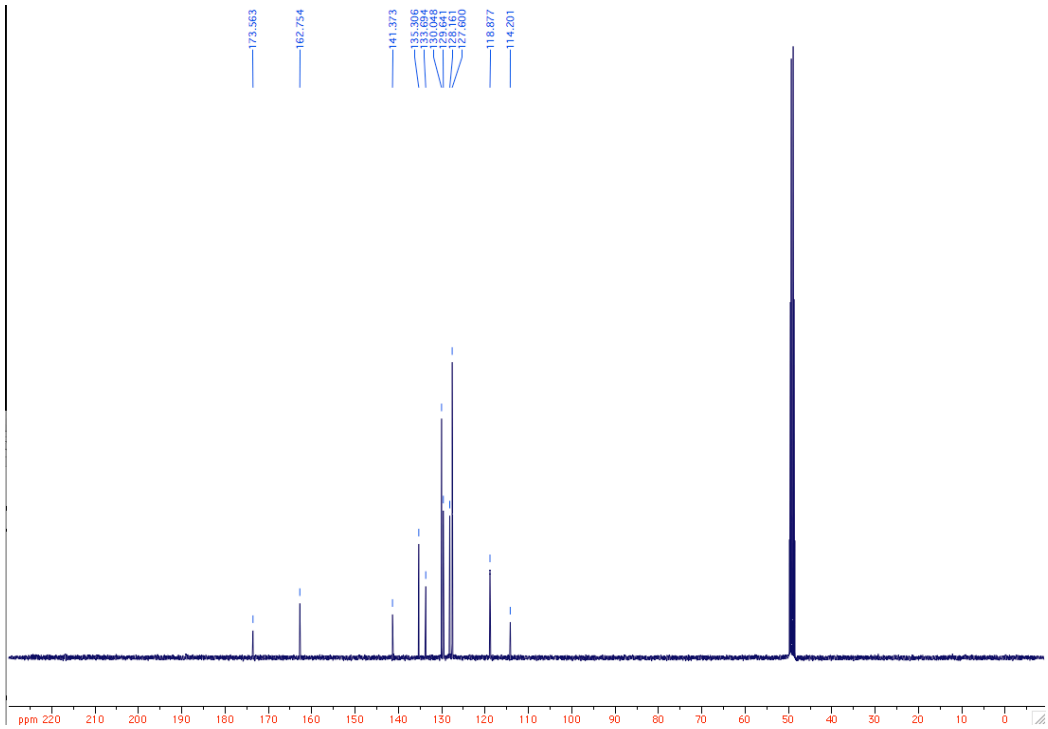

www.manaraa.com

Compound **3a**

^{1}H-NMR (CD_3OD)

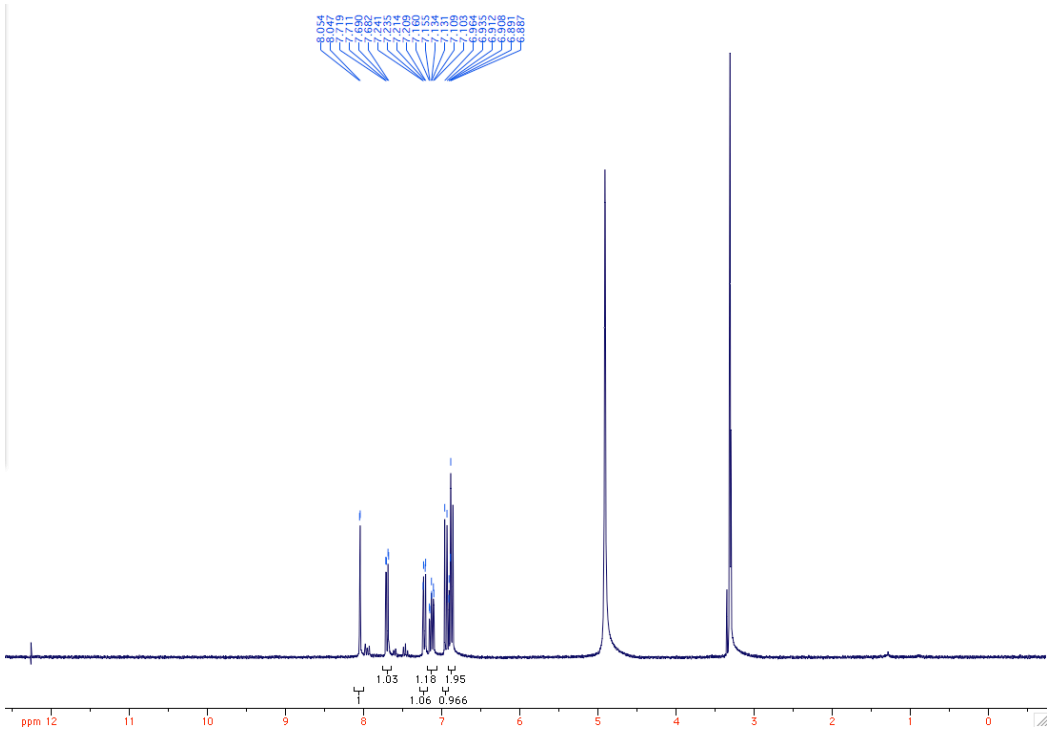

www.manaraa.com

^{13}C-NMR (CD_3OD)

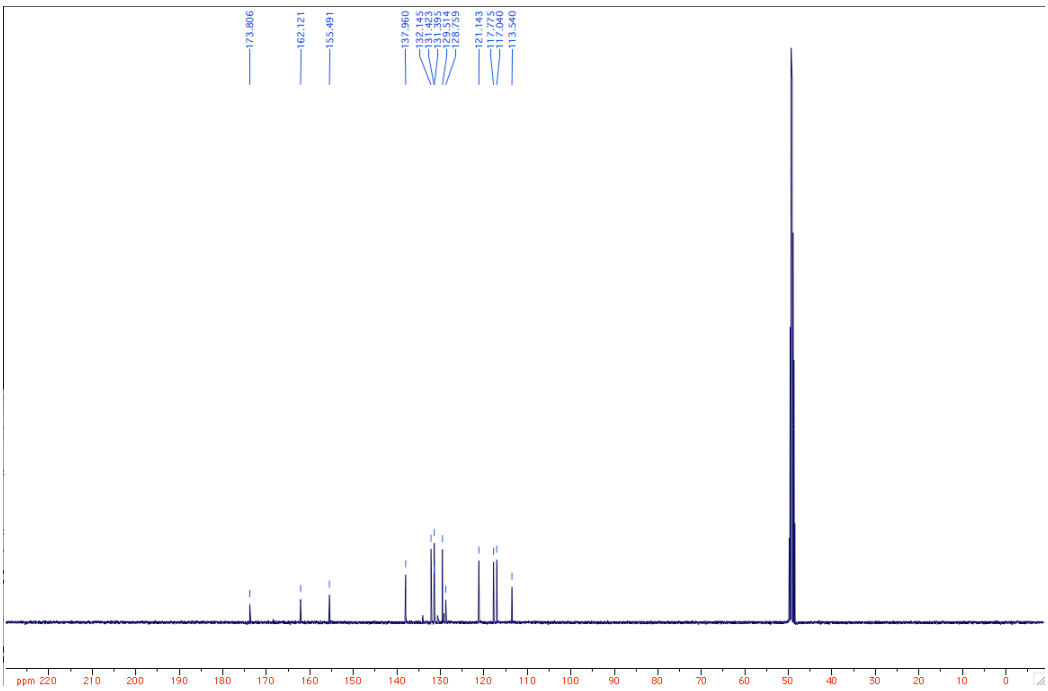

www.manaraa.com

Compound **3b**

^{1}H-NMR (CD_3OD); Identified impurities: compound **3b'**, ethyl acetate, hexanes, methanol

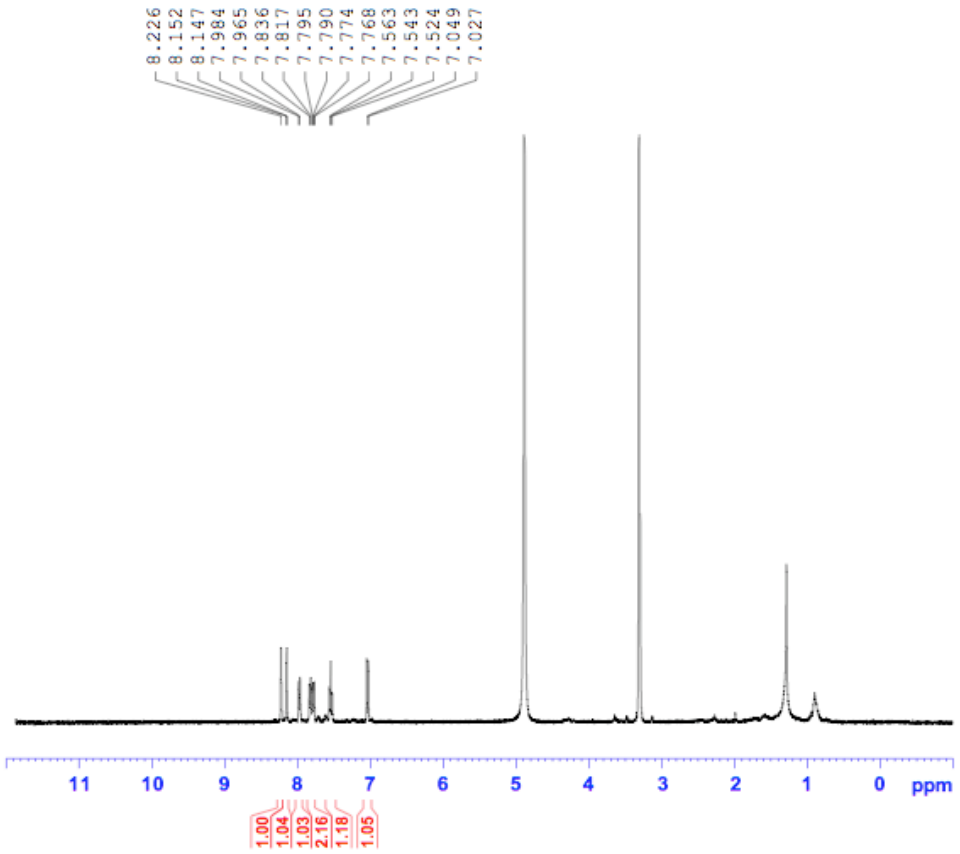

www.manaraa.com

^{13}C-NMR (CD_3OD); Identified impurities: compound **3b'**, ethyl acetate, hexanes

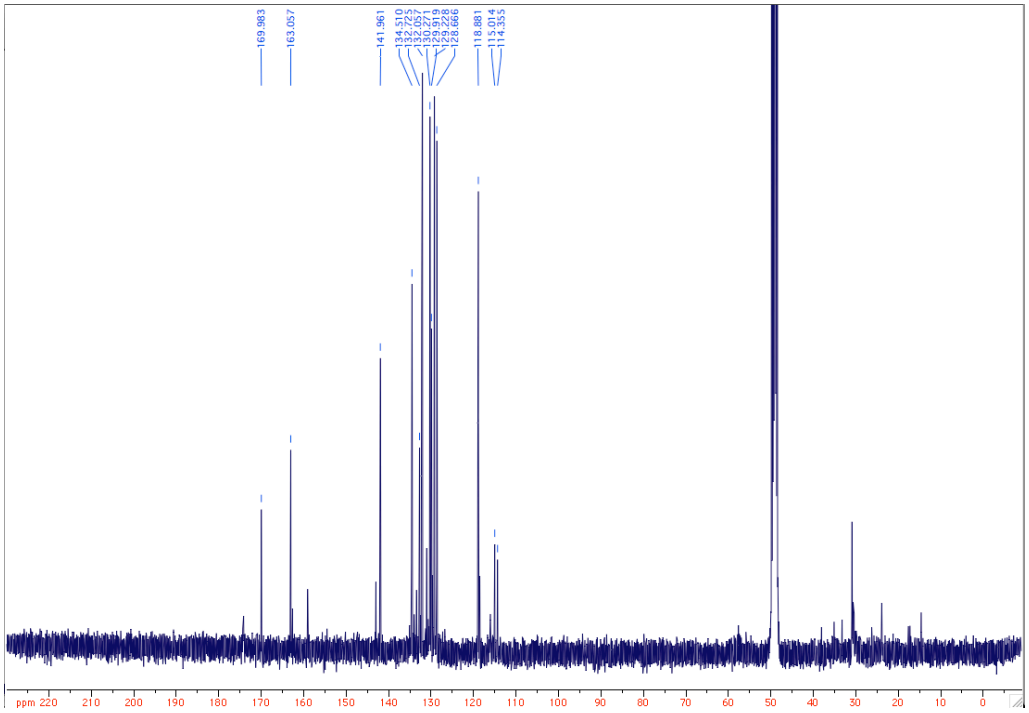

www.manaraa.com

Compound **3c**

^{1}H-NMR (CD_3OD); Identified impurities: hexanes

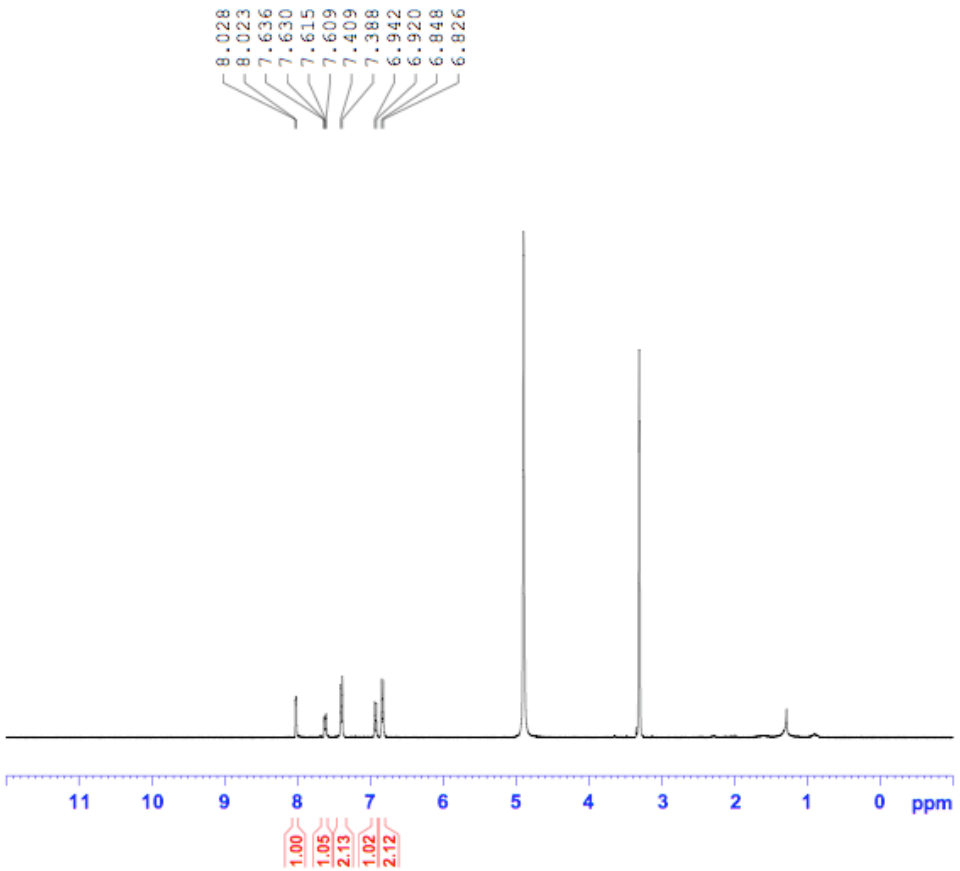

www.manaraa.com

^{13}C-NMR (CD_3OD)

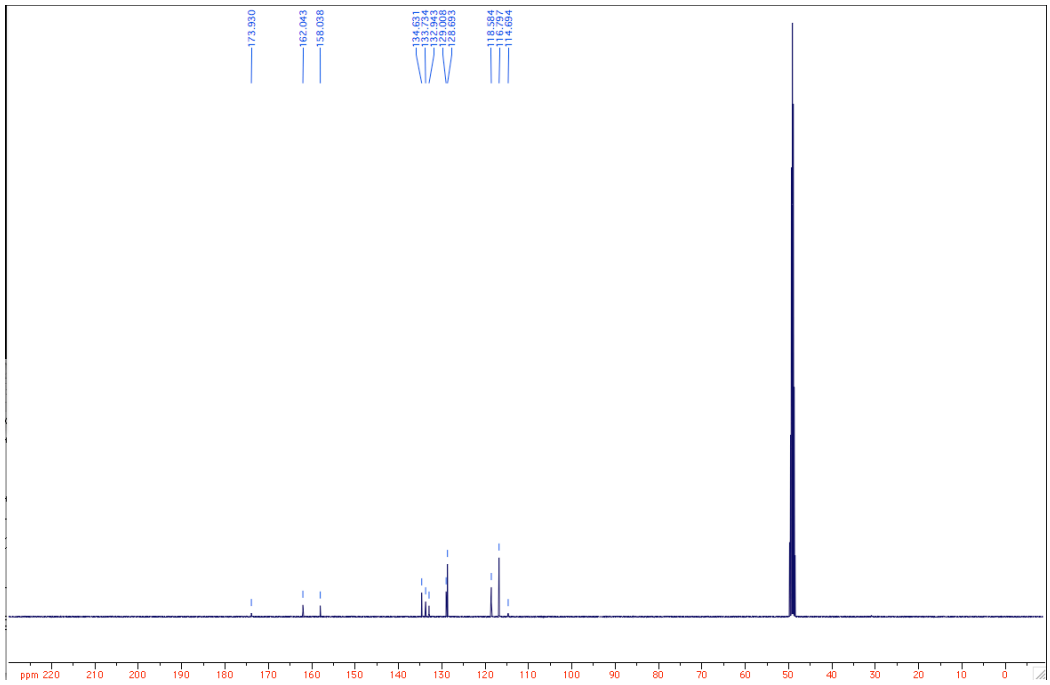

www.manaraa.com